

# 1 Differentiating between crop and soil effects on soil moisture 2 dynamics

3 Helen Scholz<sup>1</sup>, Gunnar Lischeid<sup>2,3</sup>, Lars Ribbe<sup>1</sup>, Ixchel Hernandez Ochoa<sup>4</sup>, Kathrin Grahmann<sup>2</sup>

4 <sup>1</sup>Institute for Technology and Resources Management in the Tropics and Subtropics (ITT), TH Köln, Cologne, Germany

5 <sup>2</sup>Leibniz Centre for Agricultural Landscape Research (ZALF), Müncheberg, Germany

6 <sup>3</sup>Institute for Environmental Sciences and Geography, University of Potsdam, Potsdam, Germany

7 <sup>4</sup>Institute of Crop Science and Resource Conservation (INRES), Crop Science Group, University of Bonn, Bonn, Germany

8 *Correspondence to:* kathrin.grahmann@zalf.de

9 **Abstract.** There is urgent need ~~to for~~ developing sustainable agricultural land use schemes. Intensive crop production has  
10 induced increased greenhouse gas emissions and enhanced nutrient and pesticide leaching to groundwater and streams. ~~On the~~  
11 ~~one side,~~ climate change is also expected to increase drought risk as well as the frequency of extreme precipitation events in  
12 many regions. ~~On the other side, crop production has induced increased greenhouse gas emissions and enhanced nutrient and~~  
13 ~~pesticide leaching to groundwater and receiving streams.~~ Consequently, sustainable management schemes require sound  
14 knowledge of site-specific soil hydrological processes; ~~that accounting~~ explicitly take into account for the interplay  
15 between soil heterogeneities and crops. In this study, we applied a principal component analysis to a set of 64 soil moisture  
16 time series from a diversified cropping field featuring seven distinct crops and two weeding management strategies.

17 Results showed that a about 97% of the spatial and temporal variance of the data set was explained by the first five principal  
18 components. Meteorological drivers accounted for 72.3% of the variance, 17.0% was attributed to different seasonal behaviour  
19 of different crops. While the third (4.1%) and fourth (2.2%) principal component ~~explained were interpreted as~~ effects of soil  
20 texture and cropping schemes on soil moisture variance, respectively, the effect of soil depth was represented by the fifth  
21 component (1.7%). However, neither topography nor weed control had a significant effect on soil moisture variance. Contrary  
22 to common expectations, soil and rooting pattern heterogeneity seemed not to play a major role. Findings of this study highly  
23 depend on local conditions. However, we consider the presented approach generally applicable to a large range of site  
24 conditions.

## 25 1 Introduction

26 Agriculture plays a major role to ensure the provision of food to a growing global population. At the same time, climate change  
27 is putting yield stability at risk due to extreme weather events, rising the need for sustainable management of resources, such  
28 as water and soil (Trnka et al., 2014). ~~As part of the adaptation to more challenging conditions, the transformation from large~~  
29 ~~homogeneously cropped fields towards diversified agricultural landscape was identified not only to have positive effects on~~  
30 ~~multiple ecosystem services.~~ The transformation from large homogeneously cropped fields towards diversified agricultural  
31 landscapes has been identified as an opportunity that can contribute to climate adaptation due to the positive effects on multiple

32 ecosystem services (Tamburini et al., 2020), ~~but also on the system's resilience to climatic extremes and cropping system~~  
33 resilience to climatic extremes (Birthal and Hazrana, 2019). Additionally, crop diversification is highly beneficial by reducing  
34 soil erosion through permanent soil cover (Paroda et al., 2015), and by improving resource use efficiency through wider crop  
35 rotations (Rodriguez et al., 2021).

36 In terms of soil ~~hydrological~~water dynamics, crop and management diversification can lead to improved water-stable macro-  
37 aggregation, reduced soil compaction and increased soil organic carbon, which can reduce soil water infiltration and improve  
38 water retention (Alhameid et al., 2020; Fischer et al., 2014; Karlen et al., 2006; Koudahe et al., 2022; Nunes et al., 2018).  
39 Korres et al. (2015) reported that spatial variability of soil moisture was mainly driven by soil characteristics, followed by crop  
40 cover and management. Soil moisture is also affected by soil texture and pore size distribution (Krauss et al., 2010; Rossini et  
41 al., 2021; Pan and Peters-Lidard, 2008). The quantification of the impact of these effects on soil moisture variability is  
42 important, for instance for hydrological applications and adopted management practices in agriculture (Hupet and Vanclooster,  
43 2002).

44 ~~However, as~~ the diversity of independent variables in agricultural systems increases, demands for frequency and spacing of  
45 soil moisture measurements and related data interpretation grow. Therefore, soil sensoring networks are receiving increased  
46 attention, particularly in Precision Agriculture (PA; ~~;) (Bogena et al., 2022; Salam and Raza, 2020), where the main goal is to~~  
47 increase efficiency and productivity at the farm level, while minimizing the negative impacts on the environment (Taylor and  
48 Whelan, 2010). Soil sensor networks can meaningfully contribute to PA as they can be used for various purposes, including  
49 the delineation of management zones (Khan et al., 2020; Salam and Raza, 2020). Still, one of the most important demands to  
50 be fulfilled by soil sensoring networks is soil moisture monitoring, as accurate measurement of soil water content can play an  
51 important role in improving water management and therefore, crop yields (Salam, 2020).

52 Wireless solutions, for instance based on LoRaWAN (Long Range Wide Area Network) technology, in combination with  
53 electromagnetic soil moisture sensors avoid labour-intensive and destructive soil moisture measurements that disrupt field  
54 traffic. The development of such wireless ~~soil monitoring sensor~~ networks (WSN) enables broad and affordable application  
55 also in areas with low cellular coverage (Cardell-Oliver et al., 2019; Lloret et al., 2021; Placidi et al., 2021; Prakosa et al.,  
56 2021).

57 The evolvement of ~~such systems~~WSN does not only have benefits for management but is also of high relevance for fostering  
58 the understanding of hydrological dynamics in the vadose zone. High-resolution datasets measured under real farming  
59 conditions can be used to characterize and analyse spatio-temporal dynamics of soil water. Due to the large size of data sets  
60 that are recorded with ~~wireless sensor networks~~WSN, sophisticated data analysis approaches are required to detect hidden  
61 patterns and determine influence factors on soil moisture variability (Vereecken et al., 2014). ~~Methods include geostatistical~~  
62 ~~analysis (Vereecken et al., 2014) or data driven approaches (Hong et al., 2016).~~ With the introduction of multiple-points  
63 geostatistics, it became possible to not only analyse patterns but also connect them with factors affecting soil moisture, such  
64 as topography, texture, crop growth and water uptake, and land management (Brocca et al., 2010; Strebelle et al., 2003).  
65 Wavelet analysis can analyse both localized features as well as spatial trends through which non-stationary variation of soil

66 properties can be considered (Si, 2008). Cross-correlation analysis allowed linking soil moisture variability to climatic  
67 variables (Mahmood et al., 2012). Furthermore, temporal stability analyses detect spots in the investigated area which are  
68 consistently wetter or drier than the mean soil moisture (Baroni et al., 2013; Vachaud et al., 1985, Vanderlinden et al., 2012).  
69 This method was already successfully used to detect soil moisture patterns related to soil properties, vegetation, and topography  
70 (Zhao et al., 2010).

71 Principal component analysis (PCA) is another method that was successfully applied for soil moisture variability analysis at  
72 the field (Hohenbrink et al., 2016; Hohenbrink and Lischeid, 2015; Martini et al., 2017), catchment (Korres et al., 2010;  
73 Lischeid et al., 2017; Nied et al., 2013; [Graf et al., 2014](#)), and regional (Joshi and Mohanty, 2010) scale. These studies build  
74 on previous applications in climatology where the term “Empirical Orthogonal Functions” is used (Bretherton et al., 1992) and  
75 are examples for how: Space and time dimensions can be disentangled and ~~be~~ assigned to influencing factors. Additionally,  
76 the propagation of hydrological signals (e.g. precipitation events) over depth can be assessed (Hohenbrink et al., 2016). This  
77 opens up great opportunities ~~to for contributing to improve the knowledge he knowledge of~~ changing soil ~~water hydrological~~  
78 dynamics in complex diversified agricultural systems with increasing heterogeneity (e. g. soil texture) and site-specific  
79 adjustment of crop ~~soil types~~ and field management which, to our knowledge, have hardly been studied so far.

80 ~~We~~ The main objective of this study was to identify the drivers of soil moisture variability in a diversified cropping field in  
81 terms of soil texture, crop selection and field management by applying PCA. Special focus was put on the interpretation of  
82 spatial and temporal effects of crop diversification and of soil heterogeneities on soil moisture dynamics.

83 For this, we analysed a high-resolution soil moisture data set measured by a novel underground LoRaWAN monitoring system  
84 with ~~soil moisture TDR~~ sensors in different depths of the vadose zone at a spatial-temporally diversified agricultural field in  
85 Northeast Germany. The novelty of this ~~Internet of underground Things (IoUT) soil moisture monitoring network WSN~~ relies  
86 on its is characterized by its unique on-farm installation environment. The deployment of transmission units in 0.3 m soil depth  
87 and and the deployment of 180 sensors in up to 0.9 m soil depth, allowing high spatio-temporal resolution wireless data  
88 transmission, and enabling conventional farming practices like machinery traffic, tillage and mechanical weeding. ~~The main~~  
89 ~~objective of this study was to identify the drivers of soil moisture variability in a diversified cropping field in terms of soil~~  
90 ~~texture, crop selection, soil type and field management by applying PCA. Special focus was put on the interpretation of spatial~~  
91 ~~and temporal effects of crop diversification and of soil heterogeneities on soil moisture dynamics.~~

## 92 **2 Materials and methods**

### 93 **2.1 Study site**

94 The study site (52°26'51.8"N 14°08'37.7"E, 66-83 m.a.s.l.) is located near the city of Müncheberg in the federal state of  
95 Brandenburg in Northeastern Germany. The landscape is classified as a hummocky ground moraine that formed during the  
96 last glacial periods. Glacial and interglacial processes as well as subsequent erosion resulted in highly heterogeneous soils  
97 (Deumlich et al., 2018), being classified as Dystric Podzoluvisols according to the FAO scheme (Fischer et al., 2008). In the

98 top 0.3 m soil layer, total organic carbon was 0.94% and total nitrogen content was 0.07%, and pH was 6.12. Between January  
99 1991 and December 2020, the mean annual temperature in Müncheberg was 9.6°C, and the mean annual sum of precipitation  
100 was 509 mm (DWD Climate Data Center (CDC), 2021).

## 101 **2.2 Experimental setup**

102 The data collection was carried out from December 2020 until mid of August 2021 in the patchCROP experiment (Grahmann  
103 et al, 2021; Donat et al., 2022). This landscape experiment has been set up to study the multiple effects of cropping system  
104 diversification on productivity, crop health, soil quality, and biodiversity. To that end, a cluster analysis was carried out based  
105 on soil maps and multi-year (2010 to 2019) yield data to identify high and low yield potential zones in the 70-ha large field  
106 (Donat et al., 2022). Afterwards, single experimental units comprising 30 patches with an individual size of 0.52 ha (72 m ×  
107 72 m) each, have been implemented in both, high and low yield potential zones where each of those zones is characterized by  
108 varying soil conditions and a site-specific five-year, legume-based crop rotation (Grahmann et al., 2021). The remaining area  
109 outside of the 30 patches was planted with winter rye. For the current study, twelve out of 30 patches were considered (Table  
110 1, Figure 1). Specific patches were selected to capture the soil heterogeneities in terms of soil texture, but also the seasonal  
111 patterns of the crop rotation that may have important effects on the soil water dynamics such as crop types, presence of cover  
112 crops or fallow periods. In the cropping season 2020/2021, seven different main crops were grown. For subsequent data  
113 interpretation, crops have been grouped into A) winter crops, B) fallow, followed by summer crops and C) cover crops,  
114 followed by summer crops. In seven out of twelve considered patches, weed control was carried out with herbicide application,  
115 referred as “conventional” pesticide application, while in the remaining five patches, “reduced” pesticide management was  
116 carried out by mainly using mechanical weeding, by harrowing, blind harrowing, and hoeing. Only in the case of high weed  
117 pressure herbicides were applied. Due to the potential impact of mechanical weeding, i.e., on rainwater infiltration, soil  
118 evaporation and topsoil rooting intensity, we differentiate between these modes of weed control.

## 119 **2.3 Data collection**

### 120 **2.3.1 Soil moisture data**

121 Soil moisture was recorded by a long-range-wide-area network (LoRaWAN) based ~~monitoring system~~ WSN. In each patch,  
122 one Dribox box equipped with a SDI-12 distributor (serial data interface at 1200 baud rate, TBS04, TekBox, Saigon, Vietnam)  
123 connected to six TDR-sensors (TDR310H, Acclima, Meridian, USA) and attached to an outdoor remote terminal unit (RTU)  
124 fully LoRaWAN compliant (TBS12B: 4+1 channel analogue to SDI-12 interface for 24 Bit A/D conversion of sensor signals,  
125 TekBox, Saigon, Vietnam) was installed as LoRa node. ~~The DriboxIt~~ was deployed at least 0.3 m below ground to allow  
126 ~~normal~~ field traffic and soil tillage. The sensors and boxes were installed between August and November 2020. At two  
127 georeferenced locations within each patch. At two georeferenced locations within each patch (Figure 2), TDR-soil moisture  
128 sensors were installed in 0.3, 0.6 and 0.9 m depth, respectively. Sensors were, approximately 2 m apart from the ~~Driboxes~~

129 LoRa node in angles between 45° and 60° (Figure 1). Soil moisture sensors at 0.3 m were placed horizontally, while sensors  
130 at 0.6 and 0.9 m depth were placed vertically using auger-made ~~tunnels-boreholes~~ and extension tubes for soil insertion.  
131 ~~Communication of Driboxes-LoRa nodes was wireless and ere-autarkic in-in terms of energy supply, and communication~~  
132 ~~was wireless throughout.~~ Thus, no electric cabling except from connections between sensors and ~~Driboxes-LoRa nodes~~ was  
133 needed. Under optimum conditions, battery running time of the LoRa nodes can be up to 12 months but can be reduced to 8  
134 months when radio transmission is attenuated (e.g. due to near water-saturated soil) which then increases power consumption  
135 (Bogena et al., 2009). ~~The data were~~Data was recorded every 20 minutes by the LoRa nodes through a LoRa-WAN Gateway  
136 DLOS8 (UP GmbH, Ibbenbüren, Germany) which was equipped with the modem TL-WA7510N (TP Link, Hong Kong,  
137 China) to transfer the data to a cloud from where collected data could be accessed directly after the measurement. The time  
138 series included in this study covered the period from December 01, 2020, until August 14, 2021 (Figure 2).

### 139 2.3.2 Weather data

140 Precipitation and temperature data (Figure 3) with a 15 min temporal resolution were obtained from two weather stations  
141 located in the Eastern and Western end of the main patchCROP field ~~with a 15 min temporal resolution~~. Climatic water balance  
142 was calculated from precipitation and potential evapotranspiration, both measured at the climate station by the German  
143 Weather Service in Müncheberg (DWD Climate Data Center (CDC), 2021). This station was chosen due to its proximity to  
144 the study site.

### 145 2.3.3 Remote senses data for vegetation dynamics

146 Furthermore, drone imagery from May 20, 2021, May 31, 2021, and July 06, 2021, was used for vegetation assessment. The  
147 drone fixed-wing UAV-based RS eBee platform (SenseFly Ltd., Cheseaux-Lausanne, Switzerland) was operated at noon time  
148 and recorded multispectral imagery with a Parrot Sequoia+ camera (green, red, NIR, and red edge bands, spatial resolution of  
149 0.105 m) and thermal imagery of the surface (only on May 31, 2021) with a senseFly Duet T camera with a spatial resolution  
150 of 0.091 m (Table 2). The multispectral imagery was processed with Pix4D to obtain the Normalized Difference Vegetation  
151 Index (NDVI), following Eq. (1):

$$152 \quad NDVI = \frac{NIR-Red}{NIR+Red} \quad (1)$$

153 in which NIR is the intensity of reflected near-infrared light (reflected by vegetation) and Red the intensity of reflected red  
154 light (absorbed by vegetation). A digital elevation model with a spatial resolution of 1 m (GeoBasis-DE and LGB, 2021) was  
155 used to calculate the slope (ArcGIS 10.7.0; ESRI, 2011) (Table 2).

### 156 2.3.4 Soil information

157 Soil texture by layer

158 Manual ~~classification of~~ soil texture ~~analysis~~ by layer was carried out ~~for part of the sensors~~ by ~~using~~ collecting 140 samples  
159 in eight of twelve analysed patches. Samples were taken with ~~taken with a 1 m-length~~ Pürckhauer soil auger of 1 m length in  
160 eight of twelve analysed patches. Manual sSoil textural class was ~~manually determined~~ estimated at the field by applying the  
161 protocol “Finger test to determine soil ~~types~~ texture according to DIN 19682-2 and KA5” (Sponagel et al., 2005). Additionally,  
162 representative soil samples were collected and analysed at the laboratory to determine particle size distribution for sand, silt,  
163 and clay (soil texture based on the German particle classification)-by. Soil texture was analysed following the DIN ISO 11277  
164 (2002) reference method by wet sieving and sedimentation, using the SEDIMAT 4-12 (Umwelt-Geräte-Technik GmbH,  
165 Germany). The sand fraction in this method is defined between 2 and 0.063 mm, according to IUSS Working Group WRB  
166 (2015).

167 To extrapolate the laboratory-based soil particle distribution ~~from the laboratory~~ to the ~~manual~~ soil textural classes manually  
168 determined at the field; the high and low yield potential laboratory samples were pooled separately. ~~and~~ The average soil  
169 particle distribution was calculated by for each soil textural class ~~was calculated~~ and assigned to the respective soil layer with  
170 that ~~specific~~ particular soil textural class. The soil texture analysis showed that soil texture variability increased with depth. In  
171 the third layer (average bottom depth = ~~92 cm~~ 0.92 m), the sand and clay ~~share~~ content across 133 sampling points varied  
172 between 53% to 94% and 2% to 22%, respectively. Soil ~~samples~~ sampling points were ~~between-located~~ approximately 0.8 m  
173 and 2.5 m ~~far-away~~ from the soil moisture sensors to minimize damage risk. The transferability of texture information from  
174 the sampling point to the sensor location was not ensured due to high nugget effects. Furthermore, manual soil texture analysis  
175 data were not available for all analysed patches. Consequently, they were not included into further correlation analysis.

176 Topsoil proximally sensed data

177 In October 2019, the “Geophilus” soil scanner system (Lueck and Ruehlmann, 2013) was used in the entire field to map soil  
178 electrical resistivity (ERa) of the soil as a proxy for ~~soil~~ texture for the top soil, using reference soil samples to calibrate the  
179 readings. A total of four georeferenced reference soil samples were taken until 0.25 m soil depth, and locations were selected  
180 based on the proximal soil sensor data (sensor-guided sampling; Bönecke et al., 2021). The “Geophilus” system is based on  
181 sensor fusion ~~of within which~~ ERA sensors are coupled with a ~~gamma-ray detector~~ ( $\gamma$ ) sensor. Apparent electrical conductivity  
182 was measured by pulling one or more sensor pairs mounted on wheels across the field where each pair of sensors measured a  
183 different soil depth. Amplitude and phase were measured simultaneously using frequencies from 1 MHz to 1 kHz. Reference  
184 soil samples were ~~taken in several points~~ analysed via soil-particle size analysis according to DIN ISO 11277 (2002) and  
185 served as calibration information in order to estimate sand, silt and clay content in the top 0.25 m ~~of soil for soil~~ the entire  
186 field. A non-linear regression model was applied. The RMSE of sand content (5.7%) was considerably smaller than the  
187 standard deviation of the sand content in the first layer from the manual soil texture analysis (11.9%), indicating a satisfactory  
188 prediction performance. The ~~gamma~~  $\gamma$ -sensor was used to minimize uncertainties, being less sensitive to soil moisture than the

189 ERa readings (Bönecke et al., 2021). The estimated sand content in the upper 0.25 m at the study site varied between 69.1%  
190 and 81.2% and averaged 79.0% (Table 1, Figure 1).

## 191 2.4 Data processing

192 Soil moisture data were available at 20-minute intervals. Transmission failures due to discharged batteries, signal disturbances  
193 ~~in sinks~~ after rainfall, in patches with a high density of biomass (e.g. maize), and theft of parts of the ~~monitoring system~~ WSN  
194 led to data gaps that affected in some cases all sensors of the WSN and amounted to 81 out of 257 days of the measuring  
195 period. ~~The affected days, which~~ were therefore skipped for the analysis. Whereas time series of eight sensors were excluded  
196 due to a higher frequency of transmission failures, in total, 64 time series were used for the analysis, and additional data gaps  
197 for single sensors were interpolated linearly. Of all 20,668 interpolated gaps, 96% were shorter than two hours, 3% between  
198 two and six hours and 1% longer than six hours. In 26 cases, gaps exceeded the duration of one day. The interpolation was  
199 justified as the differences between the values before and after the gaps were within the measuring accuracy of 1 vol-% of the  
200 ~~TPR~~ soil moisture sensors (Acclima Inc., 2019). As indicated by the retailer, sensors might suddenly jump to a soil moisture  
201 value of 28.6% and go back to normal again after one or few time steps. Thus, a data deletion procedure of abrupt jumps to  
202 28.6 was created. To ensure equal weighting for the subsequent analysis, all soil moisture time series were z-transformed to  
203 unit variance and zero mean each (cf. Hohenbrink and Lischeid, 2015). As a consequence, differences of absolute values were  
204 not considered by the further analysis.

## 205 2.4 Statistical analysis

206 To identify common temporal patterns among single time series, the soil moisture data set was analysed by a principal  
207 component analysis (PCA). In a first step, PCA decomposes the total variance of a multivariate data set into independent  
208 fractions called principal components (PCs). The number of PCs is the same as the number of time series in the input data set.  
209 Each PC consists of eigenvectors (loadings), scores, and eigenvalues. The scores reflect the temporal dynamics. The  
210 importance of single principal components for single sites is represented by the loadings of each PC (Jolliffe, 2002; Lehr and  
211 Lischeid, 2020). Loadings are the Pearson correlation coefficients of the single time series of the input data set with the scores  
212 of each PC, respectively. The eigenvalues of the single PC are proportional to the variance that they explain. The PCs are  
213 sorted in descending order of eigenvalues. Eigenvalues greater than one indicate that a PC explains more variance than ~~a~~  
214 single input time series could contribute to the total variance of the entire input data set (Kaiser, 1960). More details on principal  
215 component analysis for time series analysis are found in Jolliffe (2002). The PCA was performed using the *prcomp* function in  
216 R version 4.1.0 (R Development Core Team, 2021).

217 The scores of the principal components constitute time series. Every observed soil moisture z-transformed time series can be  
218 presented at arbitrary precision as a combination of various principal components. When the data set consists of time series of  
219 the same observable measured at different locations, the first principal component describes the mean behaviour inherent in  
220 the data set. Subsequent principal components reflect typical modifications of that mean behaviour at single locations due to

221 different effects. Thus, generating synthetic time series as linear combinations of the first PC and another additional PC helps  
222 to assign this additional PC to a specific effect. To that end, scores of that component have either been added to or subtracted  
223 from those of the first component using arbitrarily selected factors. The two resulting graphs show how the respective PC  
224 causes deviations from the mean behaviour of the data set.

225 The relations to soil and vegetation parameters were tested by computing the Pearson correlation coefficients between the  
226 scores and arithmetic mean values of all input time series as well as the Pearson correlation coefficients between loadings and  
227 sand content until 0.25 m depth, sensor depth, antecedent z-transformed ~~water contents~~soil moisture, slope, and drone imagery  
228 products- (NDVI and surface temperature). Eventually, the Wilcoxon-Mann-Whitney test was applied to check whether  
229 loadings can be grouped by management parameters (crops, cover crops, weeding management). All statistical analyses were  
230 conducted with R version 4.1.0 (R Development Core Team, 2021).

### 231 **3 Results**

#### 232 **3.1 Manual soil texture analysis**

233 The transferability of texture information from the sampling point to the soil moisture sensor location was not ensured due to  
234 high nugget effects. Furthermore, manual soil texture analysis data were not available for all analysed patches. Consequently,  
235 they were not included into further analysis.

#### 236 **3.2 Principal component analysis**

237 The principal component analysis yielded five components with Eigenvalues exceeding one, which accounted for >97% of the  
238 total variance of the data set (Table 3).

##### 239 **3.2.1 First principal component**

240 The first principal component explained 72.3% spatiotemporal variance of the data set. All loadings on the first PC were  
241 negative (Appendix A). The Pearson correlation coefficient of the scores of the first principal component with the mean values  
242 of all input time series was less than - 0.999 ( $p < 0.01$ ), the correlation between the scores and the cumulative climatic water  
243 balance ( $P - ET_p$ ) was -0.969 ( $p < 0.01$ ). Thus, the time series of the negative scores of this component represented the mean  
244 behaviour of soil moisture driven by external factors such as precipitation, temperature, and seasons in general which affected  
245 time series in the same way, although to different degrees (cf., Hohenbrink et al., 2016; Lischeid et al., 2021).

##### 246 **3.2.2 Second principal component**

247 The second principal component explained 17.0% of the total variance. The loadings ranged from -0.801 to 0.760 with a  
248 median of -0.030 (Figure 4). The loadings showed a crop type-group specific pattern. All winter crops (barley, oats, rye) had  
249 positive loadings with only one exception in 0.9 m depth. The summer crops maize, soy, and sunflower exhibited negative



250 loadings. In contrast, the summer crop lupine exhibited mostly positive loadings, similar to the winter crops, although of  
251 slightly smaller magnitude. According to the Wilcoxon-Mann test, the group of barley, oats, rye, and lupine differed  
252 significantly from the group of maize, soy, and sunflower.

253 As described in the Methods section, synthetic time series were generated as a linear combination of PC1 and PC2 (Figure 5).  
254 The graph resulting from applying a positive factor for PC2 represents a typical deviation from mean behaviour for sites that  
255 exhibit positive loadings, e.g., winter crops (blue line). The opposite holds for the summer crops which load negatively with  
256 PC2 (orange line). Both lines plot very close to each other in February and March. In contrast, the orange line shows lower  
257 values than the blue line in December and January, indicating lower soil moisture at the summer crop patches. The inverse  
258 holds for the subsequent summer period starting in early June, pointing to earlier and more rapid water uptake of the winter  
259 crops. In July and August, the approximately constant level of the blue curve indicates that only summer crops continue to  
260 consume water while winter crops are in their ripening phase and eventually harvested.

261 Lupine and sunflower were the summer crops which were sown first (March 30, 2021, and April 2, 2021, respectively). Maize  
262 was sown on April 16, 2021, and soy on May 15, 2021. The loadings of lupine, which were rather performing like winter crops  
263 than summer crops, indicated that lupine showed an early onset of intensive evapotranspiration, compared to other summer  
264 crops, especially sunflower which was sown at the same time.

265 For further investigation of the vegetation effect on PCs, ~~the loadings of PC2 were compared to~~ drone imagery taken at the  
266 end of May, when sowing has been completed ~~in~~ all patches, and ~~imagerys~~ taken at the beginning of July, ~~when during~~ winter  
267 crops' ~~are in the~~ ripening phase, ~~was analysed~~. The second PC's loadings of the time series from different sensors were  
268 compared to the Normalized Difference Vegetation Index (NDVI; ~~available for three dates~~) and surface temperature (only  
269 available for May 31, 2021) of the respective sensor location as a proxy for actual evapotranspiration. At the end of May, the  
270 NDVI, as a proxy for photosynthesis potential, was positively correlated with the loadings (Table 4). Surface temperature  
271 exhibited a negative correlation. The spatial pattern of surface temperature is assumed to be inversely related to that of actual  
272 evapotranspiration. Thus, both proxies, NDVI and surface temperature, support the inference that ~~in this study~~ positive loadings  
273 on this principal component represent sites with above-average plant activity and root water uptake at the end of May. This  
274 holds for sensors from all depths but was the closest for 0.9 m depth (Pearson correlation of  $r = -0.916$  for surface temperature  
275 and of  $r = 0.946$  for NDVI on May 31). The results in July compared to those in May support the observation. At the time  
276 when the winter crops are already in the ripening phase and the summer crops reach high levels of evapotranspiration, the  
277 correlations are being reversed and negative loadings indicate above-average plant activity for summer crops. On July 06,  
278 highest Pearson correlations for NDVI are found for 0.6 m depth ( $r = -0.917$ ).

### 279 **3.2.3 Third principal component**

280 The third PC explained 4.1% of the total data set's variance. Loadings ranged between -0.787 and 0.244 with a median of  
281 0.006. Extreme loadings ( $<-0.25$ ) were found only for sensors in 0.9 m depth in patches 66, 89, 95 and 102 (Figure 6). The  
282 location of these patches ~~shows a certain regional pattern, with the patches~~ roughly follow~~ings~~ an east-west direction ~~rather~~

283 ~~than showing a random location within the field. This may point to topography or soil structure causing deviations from mean~~  
284 ~~soil moisture behaviour for patches located near this gradient., which, However, this pattern cannot be assigned to topography~~  
285 ~~or structures apparent on the topsoil map (Figure 1). Loadings were closely related to the minima of the z-transformed soil~~  
286 ~~moisture in the period from December to February ( $r = 0.70$ ,  $p < 0.001$ , Figure 7). The most obvious difference between~~  
287 ~~distinguishes the orange line (negative loading on PC3) and from the blue line (positive loading on PC3) during the first half~~  
288 ~~of the study period is that the latter reaches a maximum of soil moisture after rainfall much earlier compared to the former is~~  
289 ~~the higher temporal variability and the delayed reaching of maxima in the first half of the study period~~ (Figure 8).

#### 290 **3.2.4 Fourth principal component**

291 The fourth PC explained 2.2% of the total data set's variance. The loadings were clustered by crop groups. All fallow patches  
292 showed consistent positive loadings while the patches which were covered by winter crops, showed mainly negative loadings  
293 except in patch 95 where the loadings of the two sensors in 0.3 m depth were slightly above zero (Figure 9). According to the  
294 Wilcoxon-Mann test treatment group B (fallow, followed by summer crops) differed significantly from group A (winter crops)  
295 and C (cover crops, followed by summer crops) whereas there was no significant difference between group A and C. In contrast  
296 to crop groups A and B, patches that were covered by the cover crop phacelia during the winter months, did not show one-  
297 directional loadings.

298 Figure 10 illustrates the effect of the fourth PC on time series. ~~The blue line (positive loading) shows a hydrological behaviour~~  
299 ~~which A positive factor would be typical for more sandy soils and for patches with fallow in autumn and winter (blue line). In~~  
300 ~~contrast while the orange line (negative loading) depicts behaviour that one would expect in more loamy soils and for winter~~  
301 ~~crops. The latter line exhibits slightly more due to its delayed responses to rainstorms and subsequent less steep recovery as it~~  
302 ~~would be expected for more loamy soils. The patterns in the loadings thus show a differentiation between patches with winter~~  
303 ~~crops and fallow patches in the winter months~~ (Figure 9). However, it is not clear how winter crops on the one side and fallow  
304 on the other side could induce such a different soil water behaviour shown in Figure 10.

#### 305 **3.2.5 Fifth principal component**

306 The fifth PC explained 1.7% of the data set's variance. The loadings showed a depth-related pattern. All time series from the  
307 0.3 m depth exhibited negative loadings with two minor exceptions. Whereas all time series from 0.9 m depth showed positive  
308 loadings throughout, and time series from 0.6 m depth plot in between. Loadings in 0.6 m depth and 0.9 m depth were mostly  
309 more similar to each other than to the loadings of 0.3 m depth (Figure 11). The Pearson correlation coefficient between loadings  
310 and depth was  $r = 0.710$  ( $p < 0.05$ ). Thus it can be concluded that the fifth PC reflected the effect of soil depth on soil moisture  
311 variance. This effect differed between crops, with the three most negative loadings found in maize patches while the three  
312 most positive loadings were found in lupine patches.

313 ~~The hydrological signal after rainfall events exhibits damping over depth (blue line) while sensors in the upper layer react with~~  
314 ~~a higher sensitivity (orange line) to weather conditions (Figure 10).~~

315 The soil water dynamics show a damping effect with increasing depth (Figure 12) from little damping for sensors in the upper  
316 depth (orange line) to higher damping for sensors in greater depth (blue line).  
317 Neither patterns in topography nor in weeding management modes were reflected in the loadings of PC1-PC5. Due to the lack  
318 of subsurface soil data, no additional findings could be derived from the Geophilus texture analysis.

## 319 **4 Discussion**

320 A PCA was conducted to identify the drivers of soil moisture variability in a diversified cropping field. Data consisted of  
321 observed time series from 64 soil moisture probes. Results showed that tThe first five principal components described about  
322 97% of the variance of the data set, ~~which consisted of observed time series from 64 soil moisture probes~~ and revealed various  
323 effects of weather, soil texture, soil depth, crops and management schemes (Table 3). The first principal component captured  
324 72% of the total variance. Consequently, 72% of the observed dynamics could be described by a lumped model that would not  
325 consider any within-field heterogeneity. ~~These is figure results are is~~ in the range of similar studies. ~~In the study of~~ Martini et al.  
326 (2017) ~~who found that~~ the first PC explained 58% of the variance of a data set that comprised both agricultural fields as well  
327 as grassland transects. Similarly, Lischeid et al. (2017) ascribed 70% of the variance of a forest soil hydrological moisture data  
328 set to a single component. In the study by Hohenbrink et al. (2016), 85% of the variance of soil hydrological moisture data in  
329 a set of arable field experiments with two different crop rotation schemes was attributed to the first principal component. The  
330 strong influence of weather conditions as it is shown in our study is confirmed by Choi et al. (2007) who showed that rainfall,  
331 next to topography, explained most of the surface soil moisture variability.

### 332 **4.1 Crop effects**

333 As Korres et al. (2015) stated that vegetation and management (e.g. planting and harvesting dates) are among the main causes  
334 for spatial variability of soil moisture in agricultural fields ~~besides soil parameters are vegetation and management (e.g.~~  
335 ~~planting and harvesting dates).~~ The quantification of the impact of these effects on soil moisture variability is highly important,  
336 ~~for instance for hydrological applications and adopted management practices in agriculture (Hupet and Vanclooster, 2002).~~  
337 ~~Joshi and Mohanty (2010) investigated the spatial soil moisture variability at on the field to regional scale in the Southern~~  
338 ~~Great Plains regions in the US by means of PCA and assessed the effect of vegetation as limited since none of the first seven~~  
339 ~~PC showed strong correlations with vegetation parameters. In Western China, Wang et al. (2019) used a non-linear Granger~~  
340 ~~causality framework and quantified the vegetation effect on soil moisture variability with up to 8.2%.~~ In this study, ~~conducted~~  
341 ~~at the field scale,~~ around 17% of the total variance at the field scale was attributed to the vegetation effect. When not considering  
342 the temporal component reflected by PC1 and thus only looking at the spatial variability, 61% of the remaining variance  
343 ~~(attributed to PC2 to PC64)~~ is caused by the vegetation effect reflected by PC2. Korres et al. (2010) also used PCA to identify  
344 the drivers of spatial variability of soil moisture within a cropped area but did not find such a pronounced vegetation effect. In  
345 their study, ~~more than two thirds of the spatial variability was related to soil parameters and topography.~~ In contrast, the strong

346 influence of vegetation in our study may be due to the high level of crop diversification. Within single crop fields, vegetation  
347 effects are observable due to heterogeneous biomass or root development (Brown et al., 2021; Korres et al., 2010), but may be  
348 of a lower magnitude compared to fragmented field arrangements with different crops. The high impact of crop diversification  
349 on soil moisture variability is also visible when comparing our results to the results of a field under comparable conditions in  
350 the same region with only two crop rotations in which only 3.8% was explained by the different crop rotations (Hohenbrink et  
351 al., 2016). Joshi and Mohanty (2010) investigated spatial soil moisture variability at the field to regional scale in the Southern  
352 Great Plains regions in the US by means of PCA and assessed the effect of vegetation - in contrast to this study - as limited  
353 since none of the first seven PC showed strong correlations with vegetation parameters.

354  
355 It needs to be considered that the proportion of the vegetation effect on soil moisture variability does not only vary spatially  
356 and over depth, but also over time. Under dry conditions, soil-plant interactions prevail while under moist conditions,  
357 percolation behaviour is predominant (Baroni et al., 2013). The scores are time series and reflect the effect size of a particular  
358 process represented by the respective PC. The more the scores of a certain PC deviate from zero during specific periods, the  
359 stronger the respective effect is. Consequently, the time series of PC2 scores indicates that the effect of vegetation on total  
360 variability varies by time. In accordance with literature, the absolute values of the scores of PC2, representing differences  
361 between the contrasting seasonality of crops, are highest in the dry months, May to August. This is mostly explained by the  
362 high water demand of summer crops, which are in their vegetative growth stage from May to August, whereas winter crops  
363 are already in their reproductive growth stage, including maturity, senescence and harvest where water uptake by crops is  
364 minimal or absent (Zhao et al, 2018). In the moist winter months January to March, as well as during the heavy rainfall event  
365 in July, the scores of PC2 are relatively small, showing that spatial variability at that time is caused by other factors.

366 The second principal component clearly differentiated between winter and summer crops, which was driven by the different  
367 seasonal patterns of root water uptake (Figure 4). In contrast, the fourth component differentiated between fallow followed by  
368 summer crops and winter crops, whereas phacelia followed by summer crop did not show a clear pattern-separated winter  
369 crops and fallow (Figure 9). Phacelia is grown as a cover crop and usually dies off in frost periods. Due to rather mild winter  
370 temperatures 2020/21, Phacelia was not terminated efficiently and kept growing until spring, until it was terminated  
371 mechanically. It was recently shown that the timing of removal of winter cover crops is key to provide soil water recharge for  
372 the subsequent crop, as the depletion of soil water in autumn is significant (Selzer and Schubert, 2023). Thus, some Phacelia  
373 patches exhibited negative loadings, similarly to the winter crop patches while other patches with most likely different  
374 termination dates exhibited positive loadings.

375 Hence, the fourth component obviously reflected the effect of the active root system~~plant cover~~ in the winter period,~~which~~  
376 ~~can hardly be ascribed to different patterns of root water uptake.~~ According to this component, soil moisture-water dynamics  
377 ~~at-in~~ the fallow patches mostly resembled ~~more~~ the typical behaviour ~~one would~~ expected for sandy soils, and ~~that of~~ winter  
378 crop patches showed a more damped behaviour that is usually observed in more loamy soils. Note that the term “fallow” refers  
379 to crop cover in autumn and winter only. Acharya et al. (2019) found that winter cover crops improved soil moisture from 3

380 to 5% in the top 0.3 m soil layer which is in line with the findings from Figure 10 that shows a higher water holding capacity  
381 for winter crops (orange line) in winter. However, it has also been observed that roots from winter crops can increase soil  
382 porosity and therefore, water mobility in the soil (Lange et al., 2013; Scholl et al., 2014).  
383 That feature pattern could point to a soil carbon effect on the soil's water holding capacity: Only in at the winter crop sites  
384 patches, soil organic carbon (SOC) in soil increased continuously due to root growth and root exudation, whereas  
385 mineralisation reduced SOC the organic carbon stock at in the fallow sites patches. Effects of dense living root networks on  
386 soil hydraulic conductivity have been reported, e.g., Scholl et al. (2014), Zhang et al. (2021) and Lange et al. (2013). Further  
387 soil-vegetation interactions might play a role for the delayed seepage fluxes of winter crop and part of cover crop patches, such  
388 as soil organic matter from cover crops and plant residues (Manns et al., 2014; Rossini et al., 2021). Usually, such effects are  
389 assumed to occur only at larger time scales, which is closely related to problems of detecting changes soil organic carbon  
390 (SOC) quantity or quality. So far, there is only anecdotal evidence for rather short-term soil organic carbon SOC quality  
391 affecting soil hydraulic properties even at smaller time scales. Although this effect constituted only a minor share of soil  
392 moisture variance (Table 3), it was clearly discernible as a separate principal component. This effect would be worth to be  
393 tested in more detailed future studies. If it were to be confirmed, it would be a good example for how crop management shapes  
394 soil properties.

#### 395 **4.2 Soil texture and soil depth effects**

396 ~~Texture is another highly important spatial variable that affects soil moisture. The pore size distribution, which is directly~~  
397 ~~linked to texture has great influence on wetting processes as well as on the water retention capacity of soil (Krauss et al., 2010;~~  
398 ~~Rossini et al., 2021). Furthermore, texture influences the evapotranspiration which is another main factor controlling soil~~  
399 ~~moisture (Pan and Peters Lidard, 2008). For coarse grained soils as they are present in this case study, the water retention~~  
400 ~~capacity is small, resulting in enhanced seepage fluxes (Scheffer and Schaechtel, 2002; Krauss et al. 2010).~~

401 Loadings on the third principal component were not related to crop types. In contrast, a spatial pattern emerged: Only sensors  
402 from 0.9 m depth from six adjacent patches exhibited strongly negative loadings (Figure 6), whereas all other sensors showed  
403 minor positive or negative loadings. This points to an effect of subsoil substrates, that is, higher clay content and consequently  
404 higher water holding capacity. That would be consistent with delayed response to seepage fluxes and reduced desiccation in  
405 the vegetation period (Figure 8). The strong relation between z-transformed soil moisture minima at the beginning of the study  
406 period (Figure 7) which might originate from a delayed response to a prior rainfall, at the beginning of the study period, and  
407 the regional pattern of the location of the patches following a west-east direction within the experiment might be an indicator  
408 of underlying soil structures causing this effect. Data on ~~the~~ texture at soil moisture ~~the~~ sensor locations in deeper layers would  
409 be of high value to confirm the assumptions.

410 Whereas the third principal component seems to reflect a local peculiarity, the fifth component obviously grasps a more generic  
411 feature. Loadings on this component are clearly related with depth (Figure 11). Strong positive loadings indicate a strongly  
412 damped behaviour of soil moisture time series: The blue line, representing sites with positive loadings on PC5 which is typical

413 for sensors at greater depth (Figure 12), exhibits clearly reduced amplitudes compared to the orange line, that is, sensors at  
414 shallow depth. Hohenbrink and Lischeid (2015) combined a hydrological model and principal component analysis to study the  
415 effect of soil depth and soil texture on damping of the input signal in more detail. A subsequent field study proved the relevance  
416 of that effect in a real-world setting (Hohenbrink et al., 2016). Moreover, Thomas et al. (2012) found that damping accounted  
417 for a large share of variance in a set of hydrographs from a region of 30,000 km<sup>2</sup>. Damping was also the most relevant driver  
418 of spatial variance in a set of time series of groundwater head at about the same scale (Lischeid et al., 2021).

### 419 4.3 Limitations

420 Data gaps during the studied period occurred due to multiple technical and environmental factors. Data gaps in soil moisture  
421 time series were caused by repeated temporary failure of the WSN. There was a failure of one sensor that was replaced and  
422 one LoRa node was damaged by intruding water. More relevant, however, were failures of data transmission. Yildiz et al.  
423 (2015) point to the problem of optimizing transmission power for data and acknowledgement packets depending on energy  
424 dissipation under the given conditions. E.g., saturated soil conditions and dense biomass stands reduce the transmission signal  
425 from the node to the gateway (Bogena et al., 2009). The installation of a second gateway in September 2021 increased higher  
426 transmission coverage in the field. Another obstacle was snow cover on the gateways' solar panels. Finally, solar panels were  
427 subject to theft. However, higher level of maintenance and supervision helped to reduce the number and the length of data  
428 gaps.

429  
430 PCA requires gapless time series. Gaps in single time series need to be either filled at the risk of introducing artefacts or the  
431 respective time period cannot be considered at all for analysis. This can be seen as a weakness of PCA. On the other hand, and  
432 in contrast to other time series analysis approaches, the time series need not to be equidistant. Assigning PCs to processes and  
433 effects is not straightforward and might be subject for debate. For example, in this study soil samples were taken at least at 0.8  
434 m distance from the sensors to avoid disturbance of the measurements. Due to pronounced small-scale soil variability these  
435 samples are not fully representative for the measurement sites. In spite of these limitations, the PCA results clearly point to  
436 various effects worth to be studied in more detail in subsequent studies.

### 437 **5 Conclusion**

438 ~~To disentangle and to quantify different effects of environmental processes in complex settings is a key challenge of~~  
439 ~~agricultural and environmental research. It is an indispensable prerequisite for tailored field and crop management. Mechanistic~~  
440 ~~models are a way to upscale findings from numerous single cause single effect studies. But there is urgent need to further~~  
441 ~~validate model results and to study interactions between various effects in a systematic way. Principal component analysis is~~  
442 ~~a step further to meet these challenges although not entirely without problems. In this study which focuses on the interplay~~  
443 ~~between crops and soil heterogeneities in terms of soil moisture dynamics, the strength of the methodology in contributing to~~

444 ~~disentangling different effects of complex spatially and temporally diversified cropping systems based on a comprehensive~~  
445 ~~real-world data set is presented.~~The use of PCA has a high value for the application in environmental sciences, as it contributes  
446 ~~to process understanding of soil water dynamics by disentangling the different effects of complex spatially and temporally~~  
447 ~~diversified cropping systems. In this study, M~~more than 97% of the observed spatial and temporal variance was assigned to  
448 five different effects. Meteorological drivers explained 72.3% of the total variance (PC1). Different seasonal patterns of root  
449 water uptake of winter crops compared to summer crops accounted for another 17.0% of variance (PC2). An additional share  
450 of 2.2% of variance seemed to be related to the effects of ~~a living rooting system~~~~different vegetation cover on~~ and its interplay  
451 ~~with~~ soil hydraulic properties (PC4). Heterogeneity of subsoil substrates explained 4.1 % of variance (PC3), and the damping  
452 effect of input signals ~~in the soil~~over depth another 1.7% (PC5). To summarize, plant-related direct and indirect effects  
453 accounted for 19.2% of the variance (PC2 and PC4), and soil-related effects only for 5.8% (PC3 and PC5). In particular, the  
454 plant-induced effects on soil hydraulic properties would be worthwhile to be studied in more detail.

455 ~~Findings of this study highly depend on local conditions. However, the methodology itself is generally applicable to other site~~  
456 ~~conditions and can lead to improved management practices through improved knowledge about soil water dynamics.~~  
457 ~~Furthermore, information from this study can also help to develop both parsimonious and tailored mechanistic models for~~  
458 ~~model upscaling. In this regard, principal component analysis of large soil moisture data sets from real-world monitoring setups~~  
459 ~~performed a meaningful diagnostic tool for complex cropping systems.~~

460 ~~Knowledge from data-driven approaches can support adequate crop selection as a management option to encounter the~~  
461 ~~increasing drought risk in the study region. It has been shown that principal component analysis has a high value for the~~  
462 ~~application in environmental sciences, as it allows to draw conclusions about variabilities in large data sets from real world~~  
463 ~~monitoring setups despite gaps in time series. Information from this study will contribute to elucidate management effects as~~  
464 ~~well as to develop both parsimonious and tailored mechanistic models. Findings of this study highly depend on local~~  
465 ~~conditions. However, we consider the presented approach generally applicable to a large range of site conditions. In this regard,~~  
466 ~~principal component analysis of soil moisture time series performed as a powerful diagnostic tool and is highly recommended.~~

## 467 **Acknowledgments**

468 The maintenance of the patchCROP experimental infrastructure and the LoRaWAN soil sensor system is ensured by the  
469 Leibniz Centre for Agricultural Landscape Research. The authors acknowledge the additional support from the German  
470 Research Foundation under Germany's Excellence Strategy, EXC-2070 – 390732324 – PhenoRob for patchCROP related  
471 research activities.

472 The authors thank Gerhard Kast, Thomas von Oepen, Lars Richter, Robert Zieciak, Sigrid Ehlert and Motaz Abdelaziz for  
473 their dedicated support in maintenance of the monitoring system and data collection.

474 **Competing interests**

475 The authors declare that they have no conflict of interest.

476 **References**

477 Acclima Inc.: True TDR310H. Soil-Water-Temperature-BEC-Sensor, 2019.

478 [Acharya, B. S., Dodla, S., Gaston, L. A., Darapuneni, M., Wang, J. J., Sepat, S., and Bohara, H.: Winter cover crops effect on soil moisture and soybean growth and yield under different tillage systems, Soil and Tillage Research, 195, <https://doi.org/10.1016/j.still.2019.104430>, 2019.](#)

481 Alhameid, A., Singh, J., Sekaran, U., Ozlu, E., Kumar, S., and Singh, S.: Crop rotational diversity impacts soil physical and hydrological properties under long-term no- and conventional-till soils, *Soil Res.*, 58, 84, <https://doi.org/10.1071/SR18192>, 2020.

484 Baroni, G., Ortuani, B., Facchi, A., and Gandolfi, C.: The role of vegetation and soil properties on the spatio-temporal variability of the surface soil moisture in a maize-cropped field, *Journal of Hydrology*, 489, 148–159, <https://doi.org/10.1016/j.jhydrol.2013.03.007>, 2013.

487 BIRTHAL, P. S. and HAZRANA, J.: Crop diversification and resilience of agriculture to climatic shocks: Evidence from India, *Agricultural Systems*, 173, 345–354, <https://doi.org/10.1016/j.agsy.2019.03.005>, 2019.

489 [Bogena, H. R., Huisman, J. A., Meier, H., and Weuthen, A.: Hybrid wireless underground sensor networks: Quantification of signal attenuation in soil, Vadose Zone J., 8, 755-761, <https://doi.org/10.2136/vzj2008.0138>, 2009.](#)

491 Bogena, H. R., Weuthen, A., and Huisman, J. H.: Recent Developments in Wireless Soil Moisture Sensing to Support Scientific Research and Agricultural Management, *Sensors*, 22, 9792, <https://doi.org/10.3390/s22249792>, 2022.

493 Bönecke, E., Meyer, S., Vogel, S., Schröter, I., Gebbers, R., Kling, C., Kramer, E., Lück, K., Nagel, A., Philipp, G., Gerlach, F., Palme, S., Scheibe, D., Zieger, K., Rühlmann, J.: Guidelines for precise lime management based on high-resolution soil pH, texture and SOM maps generated from proximal soil sensing data, *Precision Agric*, 22, 493-523, <https://doi.org/10.1007/s11119-020-09766-8>, 2021.

497 Bretherton, C. S., Smith, C., and Wallace, J. M.: An intercomparison of methods for finding coupled patterns in climate data, *Journal of Climatology*, 5, 541–560, 1992.

499 Brocca, L., Melone, F., Moramarco, T., and Morbidelli, R.: Spatial-temporal variability of soil moisture and its estimation across scales, *Water Resour. Res.*, 46, <https://doi.org/10.1029/2009WR008016>, 2010.

501 Brown, M., Heinse, R., Johnson-Maynard, J., and Huggins, D.: Time-lapse mapping of crop and tillage interactions with soil water using electromagnetic induction, *Vadose zone j.*, 20, <https://doi.org/10.1002/vzj2.20097>, 2021.

503 Cardell-Oliver, R., Hübner, C., Leopold, M., and Beringer, J.: Dataset: LoRa Underground Farm Sensor Network, in: Proceedings of the 2nd Workshop on Data Acquisition To Analysis - DATA'19, the 2nd Workshop, New York, NY, USA, 26–28, <https://doi.org/10.1145/3359427.3361912>, 2019.

506 [Choi, M., Jacobs, J. M., and Cosh, M. H.: Scaled spatial variability of soil moisture fields, Geophys. Res. Lett., 34, <https://dx.doi.org/10.1029/2006GL028247>, 2007.](#)



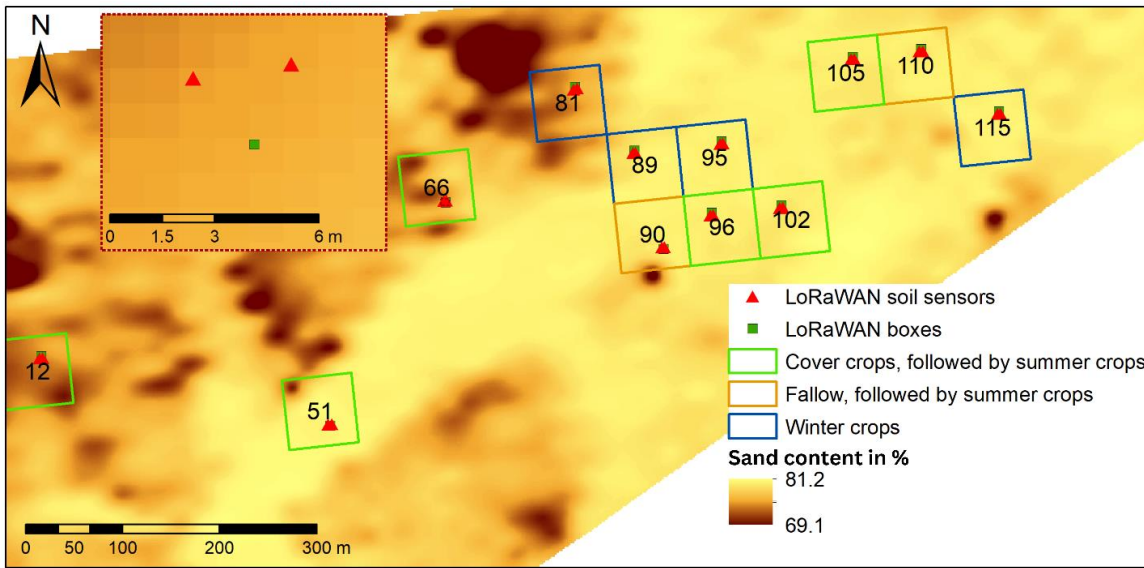
- 508 Deumlich, D., Ellerbrock, R. H., and Frielinghaus, Mo.: Estimating carbon stocks in young moraine soils affected by erosion,  
509 CATENA, 162, 51–60, <https://doi.org/10.1016/j.catena.2017.11.016>, 2018.
- 510 Donat, M., Geistert, J., Grahmann, K., Bloch, R., and Bellingrath-Kimura, S. D.: Patch cropping- a new methodological  
511 approach to determine new field arrangements that increase the multifunctionality of agricultural landscapes, Computers and  
512 Electronics in Agriculture, 197, 106894, <https://doi.org/10.1016/j.compag.2022.106894>, 2022.
- 513 [DIN ISO 11277: Soil quality - Determination of particle size distribution in mineral soil material - Method by sieving and  
514 sedimentation \(ISO 11277:1998 + ISO 11277:1998 Corrigendum 1:2002\), Beuth-Verlag, Berlin,  
515 https://dx.doi.org/10.31030/9283499, 2002.](https://dx.doi.org/10.31030/9283499)
- 516 DWD Climate Data Center (CDC): Historische tägliche Stationsbeobachtungen (Temperatur, Druck, Niederschlag,  
517 Sonnenscheindauer, etc.) für Deutschland, Version v21.3, 2021.
- 518 Fischer, C., Roscher, C., Jensen, B., Eisenhauer, N., Baade, J., Attinger, S., Scheu, S., Weisser, W. W., Schumacher, J.,  
519 Hildebrandt, A.: How Do Earthworms, Soil Texture and Plant Composition Affect Infiltration along an Experimental Plant  
520 Diversity Gradient in Grassland?, PLoS ONE, 9, 6, <https://doi.org/10.1371/journal.pone.0098987>, 2014.
- 521 Fischer, G. F., Nachtergaele, S., Prieler, S., van Velthuizen, H. T., Verelst, L., and Wisberg, D.: Global Agro-ecological Zones  
522 Assessment for Agriculture (GAEZ 2008), IIASA, Laxenburg, Austria and FAO, Rome, 2008.
- 523 GeoBasis-DE and Landesvermessung und Geobasisinformation Brandenburg (LGB): Digitales Geländemodell (DGM),  
524 Landesvermessung und Geobasisinformation Brandenburg (LGB), Potsdam, 2021.
- 525 [Graf, A., Bogena, H. R., Drüe, C., Herdelauf, H., Pütz, T., Heinemann, G., and Vereecken, H.: Spatiotemporal relations  
526 between water budget components and soil water content in a forested tributary catchment, Water Resour. Res., 50, 4837-  
527 4857, https://doi.org/10.1002/2013WR014516, 2014.](https://doi.org/10.1002/2013WR014516)
- 528 Grahmann, K., Reckling, M., Hernandez-Ochoa, I., and Ewert, F.: An agricultural diversification trial by patchy field  
529 arrangements at the landscape level: The landscape living lab “patchCROP,” in: Aspects of Applied Biology, Intercropping  
530 for sustainability: Research developments and their application, 385–391, 2021.
- 531 Hohenbrink, T. L. and Lischeid, G.: Does textural heterogeneity matter? Quantifying transformation of hydrological signals  
532 in soils, Journal of Hydrology, 523, 725–738, <https://doi.org/10.1016/j.jhydrol.2015.02.009>, 2015.
- 533 Hohenbrink, T. L., Lischeid, G., Schindler, U., and Hufnagel, J.: Disentangling the Effects of Land Management and Soil  
534 Heterogeneity on Soil Moisture Dynamics, Vadose Zone Journal, 15, <https://doi.org/10.2136/vzj2015.07.0107>, 2016.
- 535 ~~Hong, Z., Kalbaczek, Z., Iyer, R. K.: A Data Driven Approach to Soil Moisture Collection and Prediction, 2016 IEEE  
536 International Conference on Smart Computing (SMARTCOMP), St. Louis, MO, USA, 1-6,  
537 https://doi.org/10.1109/SMARTCOMP.2016.7501673, 2016.~~
- 538 Hupet, F. and Vanclooster, M.: Intraseasonal dynamics of soil moisture variability within a small agricultural maize cropped  
539 field, Journal of Hydrology, 261, 86–101, 2002.
- 540 [IUSS Working Group WRB: World Reference Base for Soil Resources 2014, Update 2015, International Soil Classification  
541 System for Naming Soils and Creating Legends for Soil Maps, World Soil Resources Reports No. 106, Rome: FAO, 2015.](https://doi.org/10.1016/j.geoderma.2014.07.010)
- 542 Jolliffe, I. T.: Principal component analysis. Springer Series in Statistics, Springer, New York, 2002.

- 543 Joshi, C. and Mohanty, B. P.: Physical controls of near-surface soil moisture across varying spatial scales in an agricultural  
544 landscape during SMEX02: Physical controls of soil moisture, *Water Resour. Res.*, 46,  
545 <https://doi.org/10.1029/2010WR009152>, 2010.
- 546 Kaiser, H. F.: The Application of Electronic Computers to Factor Analysis, *Educ. Psychol. Measur.*, 20,  
547 <https://doi.org/10.1177/001316446002000116>, 1960.
- 548 Karlen, D. L., Hurley, E. G., Andrews, S. S., Cambardella, C. A., Meek, D. W., Duffy, M. D., and Mallarino, A. P.: Crop  
549 Rotation Effects on Soil Quality at Three Northern Corn/Soybean Belt Locations, *Agron.j.*, 98, 484–495,  
550 <https://doi.org/10.2134/agronj2005.0098>, 2006.
- 551 Khan, H., Farooque, A. A., Acharya, B., Abbas, F., Esau, T. J., and Zaman, Q. U.: Delineation of Management Zones for Site-  
552 Specific Information about Soil Fertility Characteristics through Proximal Sensing of Potato Fields, *Agronomy*, 10, 1854,  
553 <https://doi.org/10.3390/agronomy10121854>, 2020.
- 554 Korres, W., Koyama, C. N., Fiener, P., and Schneider, K.: Analysis of surface soil moisture patterns in agricultural landscapes  
555 using Empirical Orthogonal Functions, *Hydrol. Earth Syst. Sci.*, 14, 751–764, <https://doi.org/10.5194/hess-14-751-2010>, 2010.
- 556 Korres, W., Reichenau, T. G., Fiener, P., Koyama, C. N., Bogena, H. R., Cornelissen, T., Baatz, R., Herbst, M., Diekkrüger,  
557 B., Vereecken, H., and Schneider, K.: Spatio-temporal soil moisture patterns – A meta-analysis using plot to catchment scale  
558 data, *Journal of Hydrology*, 520, 326–341, <https://doi.org/10.1016/j.jhydrol.2014.11.042>, 2015.
- 559 Koudahe, K., Allen, S. C., Djaman, K.: Critical review of the impact of cover crops on soil properties, *International Soil and*  
560 *Water Conservation Research*, 10, 343-354, <https://doi.org/10.1016/j.iswcr.2022.03.003>, 2022.
- 561 Krauss, L., Hauck, C., and Kottmeier, C.: Spatio-temporal soil moisture variability in Southwest Germany observed with a  
562 new monitoring network within the COPS domain, *metz*, 19, 523–537, <https://doi.org/10.1127/0941-2948/2010/0486>, 2010.
- 563 Lange, B., Germann, P. F., and Lüscher, P.: Greater abundance of *Fagus sylvatica* in coniferous flood protection forests due  
564 to climate change: impact of modified root densities on infiltration, *Eur J Forest Res*, 132, 151–163,  
565 <https://doi.org/10.1007/s10342-012-0664-z>, 2013.
- 566 Lehr, C. and Lischeid, G.: Efficient screening of groundwater head monitoring data for anthropogenic effects and measurement  
567 errors, *Hydrol. Earth Syst. Sci.*, 24, 501–513, <https://doi.org/10.5194/hess-24-501-2020>, 2020.
- 568 Lischeid, G., Frei, S., Huwe, B., Bogner, C., Lüers, J., Babel, W., and Foken, T.: Catchment Evapotranspiration and Runoff,  
569 in: *Energy and Matter Fluxes of a Spruce Forest Ecosystem*, vol. 229, Springer, Cham, Cham, 355–375, 2017.
- 570 Lischeid, G., Dannowski, R., Kaiser, K., Nützman, G., Steidl, J., and Stüve, P.: Inconsistent hydrological trends do not  
571 necessarily imply spatially heterogeneous drivers, *Journal of Hydrology*, 596, 126096,  
572 <https://doi.org/10.1016/j.jhydrol.2021.126096>, 2021.
- 573 Lloret, J., Sendra, S., Garcia, L., and Jimenez, J. M.: A Wireless Sensor Network Deployment for Soil Moisture Monitoring  
574 in Precision Agriculture, *Sensors*, 21, 7243, <https://doi.org/10.3390/s21217243>, 2021.
- 575 Lueck, E. and Ruehlmann, J.: Resistivity mapping with *Geophilus Electricus* - Information about lateral and vertical soil  
576 heterogeneity, *Geoderma*, 199, 2–11, <https://doi.org/10.1016/j.geoderma.2012.11.009>, 2013.
- 577 Mahmood, R., Littell, A., Hubbard, K. G., and You, J.: Observed data-based assessment of relationships among soil moisture  
578 at various depths, precipitation, and temperature, *Applied Geography*, 34, 255–264,  
579 <https://doi.org/10.1016/j.apgeog.2011.11.009>, 2012.

- 580 Martini, E., Wollschläger, U., Musolff, A., Werban, U., and Zacharias, S.: Principal Component Analysis of the Spatiotemporal  
581 Pattern of Soil Moisture and Apparent Electrical Conductivity, *Vadose Zone Journal*, 16, vzj2016.12.0129,  
582 <https://doi.org/10.2136/vzj2016.12.0129>, 2017.
- 583 Nied, M., Hundecha, Y., and Merz, B.: Flood-initiating catchment conditions: a spatio-temporal analysis of large-scale soil  
584 moisture patterns in the Elbe River basin, *Hydrol. Earth Syst. Sci.*, 17, 1401–1414, <https://doi.org/10.5194/hess-17-1401-2013>,  
585 2013.
- 586 Nunes, M. R., van Es, H. M., Schindelbeck, R., Ristow, A. J., Ryan, M.: No-till and cropping system diversification improve  
587 soil health and crop yield, *Geoderma*, 328, 30-43, <https://doi.org/10.1016/j.geoderma.2018.04.031>, 2018.
- 588 Pan, F. and Peters-Lidard, C. D.: On the Relationship Between Mean and Variance of Soil Moisture Fields, *JAWRA Journal*  
589 of the American Water Resources Association, 44, 235–242, <https://doi.org/10.1111/j.1752-1688.2007.00150.x>, 2008.
- 590 Paroda, Raj. S., Suleimenov, M., Yusupov, H., Kireyev, A., Medeubayev, R., Martynova, L., and Yusupov, K.: Crop  
591 Diversification for Dryland Agriculture in Central Asia, in: *CSSA Special Publications*, edited by: Rao, S. C. and Ryan, J.,  
592 Crop Science Society of America and American Society of Agronomy, Madison, WI, USA, 139–150,  
593 <https://doi.org/10.2135/cssaspecpub32.c9>, 2015.
- 594 Placidi, P., Morbidelli, R., Fortunati, D., Papini, N., Gobbi, F., and Scorzoni, A.: Monitoring Soil and Ambient Parameters in  
595 the IoT Precision Agriculture Scenario: An Original Modeling Approach Dedicated to Low-Cost Soil Water Content Sensors,  
596 *Sensors*, 21, 5110, <https://doi.org/10.3390/s211155110>, 2021.
- 597 Prakosa, S. W., Faisal, M., Adhitya, Y., Leu, J.-S., Köppen, M., and Avian, C.: Design and Implementation of LoRa Based  
598 IoT Scheme for Indonesian Rural Area, *Electronics*, 10, 77, <https://doi.org/10.3390/electronics10010077>, 2021.
- 599 R Development Core Team: R: A Language and Environment for Statistical Computing, R Foundation for Statistical  
600 Computing (Version 4.1.0, <http://www.R-project.org>), Vienna, 2021.
- 601 Rodriguez, C., Mårtensson, L.-M. D., Jensen, E. S., and Carlsson, G.: Combining crop diversification practices can benefit  
602 cereal production in temperate climates, *Agron. Sustain. Dev.*, 41, 48, <https://doi.org/10.1007/s13593-021-00703-1>, 2021.
- 603 Rossini, P. R., Ciampitti, I. A., Hefley, T., and Patrignani, A.: A soil moisture-based framework for guiding the number and  
604 location of soil moisture sensors in agricultural fields, *Vadose zone J.*, 20, <https://doi.org/10.1002/vzj2.20159>, 2021.
- 605 Salam, A.: *Internet of Things for Sustainable Community Development: Wireless Communications, Sensing, and Systems*,  
606 Springer International Publishing, Cham, Switzerland, <https://doi.org/10.1007/978-3-030-35291-2>, 2020.
- 607 Salam, A. and Raza, U.: *Signals in the Soil: Developments in Internet of Underground Things*, Springer International  
608 Publishing, Cham, Switzerland, <https://doi.org/10.1007/978-3-030-50861-6>, 2020.
- 609 Scheffer, F. and Schachtschabel, P.: *Lehrbuch der Bodenkunde*, 15th ed., Spektrum Akademischer Verlag GmbH. Berlin,  
610 Heidelberg, <https://doi.org/10.1007/978-3-662-55871-3>, 2002.
- 611 Scholl, P., Leitner, D., Kammerer, G., Loiskandl, W., Kaul, H.-P., and Bodner, G.: Root induced changes of effective 1D  
612 hydraulic properties in a soil column, *Plant Soil*, 381, 193–213, <https://doi.org/10.1007/s11104-014-2121-x>, 2014.
- 613 *Selzer, T., and Schubert, S.: Water dynamics of cover crops: No evidence for relevant water input through occult precipitation,*  
614 *J Agro Crop Sci.*, 209, 422-437, <https://doi.org/10.1111/jac.12631>, 2023.
- 615 Si, B. C.: Spatial Scaling Analyses of Soil Physical Properties: A Review of Spectral and Wavelet Methods, *Vadose Zone*  
616 *Journal*, 7, 547–562, <https://doi.org/10.2136/vzj2007.0040>, 2008.

- 617 Sponagel, H., Grotenthaler, W., Hartmann, K.J., Hartwich, R., Janetzko, P., Joisten, H., Kühn, D., Sabel, K.J., Traidl, R.  
618 (Eds.): *Bodenkundliche Kartieranleitung (German Manual of Soil Mapping, KA5)*, 5<sup>th</sup> edition, Bundesanstalt für  
619 Geowissenschaften und Rohstoffe, Hannover, 2005.
- 620 Strebelle, S., Payrazyan, K., and Caers, J.: Modeling of a Deepwater Turbidite Reservoir Conditional to Seismic Data Using  
621 Principal Component Analysis and Multiple-Point Geostatistics, *SPE Journal*, 8, 227–235, <https://doi.org/10.2118/85962-PA>,  
622 2003.
- 623 Tamburini, G., Bommarco, R., Wanger, T. C., Kremen, C., van der Heijden, M. G. A., Liebman, M., and Hallin, S.:  
624 Agricultural diversification promotes multiple ecosystem services without compromising yield, *Sci. Adv.*, 6, eaba1715,  
625 <https://doi.org/10.1126/sciadv.aba1715>, 2020.
- 626 Taylor, J. and Whelan, B.: *A General Introduction to Precision Agriculture*, 2010.
- 627 Thomas, B., Lischeid, G., Steidl, J., and Dannowski, R.: Regional catchment classification with respect to low flow risk in a  
628 Pleistocene landscape, *Journal of Hydrology*, 475, 392–402, <https://doi.org/10.1016/j.jhydrol.2012.10.020>, 2012.
- 629 Trnka, M., Rötter, R. P., Ruiz-Ramos, M., Kersebaum, K. C., Olesen, J. E., Žalud, Z., and Semenov, M. A.: Adverse weather  
630 conditions for European wheat production will become more frequent with climate change, *Nature Clim Change*, 4, 637–643,  
631 <https://doi.org/10.1038/nclimate2242>, 2014.
- 632 Vachaud, G., Passerat De Silans, A., Balabanis, P., Vauclin, M.: Temporal Stability of Spatially Measured Soil Water  
633 Probability Density Function, *Soil Science Society of America Journal*, 49, 822-828,  
634 <https://doi.org/10.2136/sssaj1985.03615995004900040006x>, 1985.
- 635 Vanderlinden, K., Vereecken, H., Hardelauf, H., Herbst, M., Martínez, G., Cosh, M. H., Pachepsky, Y. A.: Temporal Stability  
636 of Soil Water Contents: A Review of Data and Analyses, *Vadose Zone Journal*, <https://doi.org/10.2136/vzj2011.0178>, 2012.
- 637 Vereecken, H., Huisman, J. A., Pachepsky, Y., Montzka, C., van der Kruk, J., Bogaen, H., Weihermüller, L., Herbst, M.,  
638 Martínez, G., and Vanderborght, J.: On the spatio-temporal dynamics of soil moisture at the field scale, *Journal of Hydrology*,  
639 516, 76–96, <https://doi.org/10.1016/j.jhydrol.2013.11.061>, 2014.
- 640 ~~Wang, Y., Yang, J., Chen, Y., Fang, G., Duan, W., Li, Y., and De Maeyer, P.: Quantifying the Effects of Climate and~~  
641 ~~Vegetation on Soil Moisture in an Arid Area, China, *Water*, 11, 767, <https://doi.org/10.3390/w11040767>, 2019.~~
- 642 Yang, L., Chen, L., and Wei, W.: Effects of vegetation restoration on the spatial distribution of soil moisture at the hillslope  
643 scale in semi-arid regions, *CATENA*, 124, 138–146, <https://doi.org/10.1016/j.catena.2014.09.014>, 2015.
- 644 ~~Yildiz, H. U., Tavli, B., and Yanikomeroglu, H.: Transmission power control for link-level handshaking in wireless sensor~~  
645 ~~networks, *IEEE Sensors Journal*, 16, 2, 561-576. 2015.~~
- 646 ~~Zhang, J., Li, Y., Yang, T., Liu, D., Liu, X., and Jiang, N.: Spatiotemporal variation of moisture in rooted soil, *CATENA*, 200,~~  
647 ~~105144, <https://doi.org/10.1016/j.catena.2021.105144>, 2021.~~
- 648 ~~Zhao, X., Li, F., Ai, Z., Li, J., and Gu, C.: Stable isotope evidences for identifying crop water uptake in a typical winter wheat–~~  
649 ~~summer maize rotation field in the North China Plain, *Science of The Total Environment*, 618, 121-131,~~  
650 ~~<https://doi.org/10.1016/j.scitotenv.2017.10.315>, 2018.~~
- 651 Zhao, Y., Peth, S., Wang, X. Y., Lin, H., and Horn, R.: Controls of surface soil moisture spatial patterns and their temporal  
652 stability in a semi-arid steppe, *Hydrol. Process.*, 24, 2507–2519, <https://doi.org/10.1002/hyp.7665>, 2010.

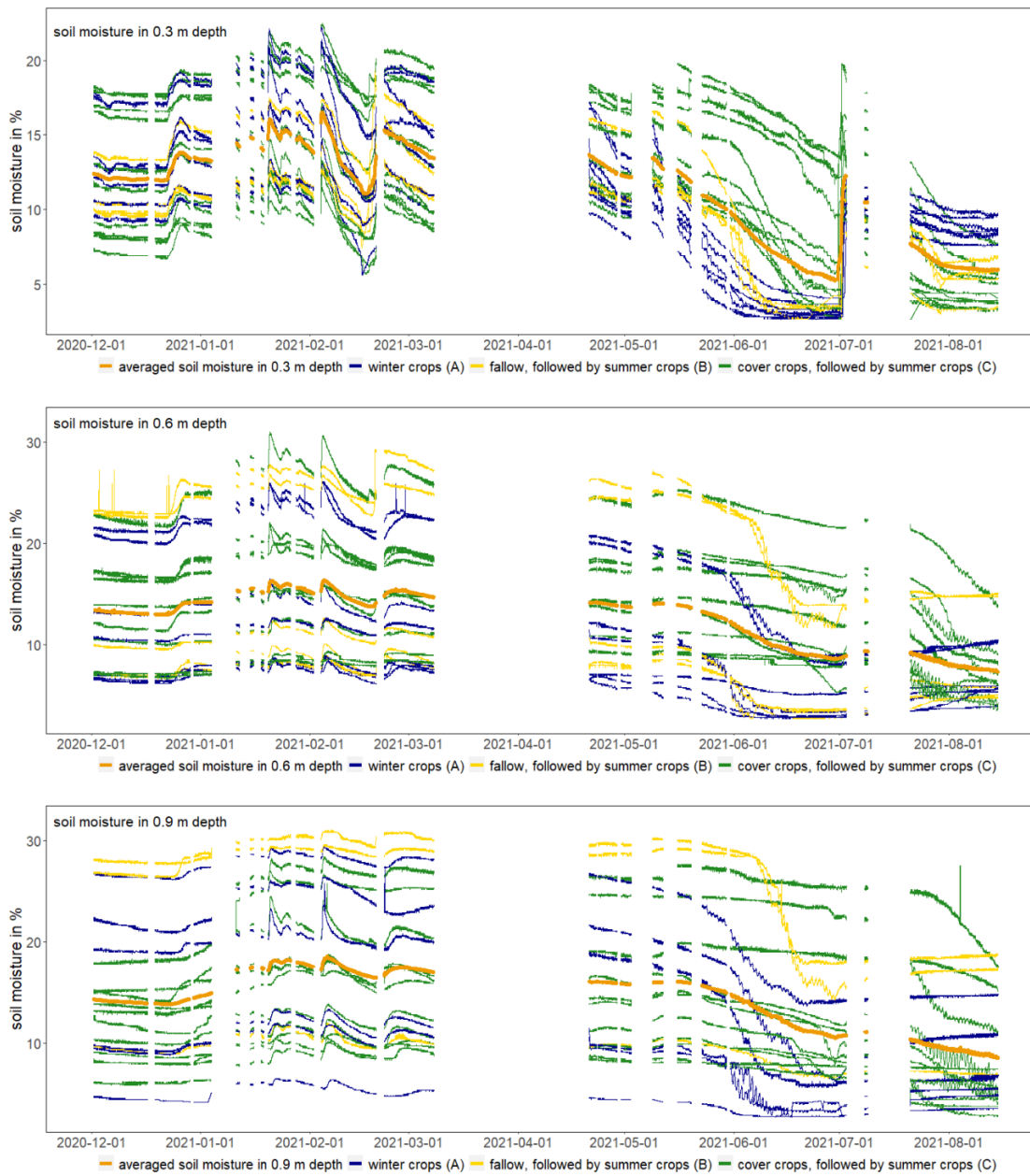
## 653 **Figures and Tables**



654

655 **Figure 1: Sand content (in %) in the top 0.25 m soil depth, and location of the analysed patches, including soil sensors**  
 656 **(triangle) and boxes (square) under different crop rotations at the patchCROP landscape laboratory, patchCROP, Tempelberg,**  
 657 **Brandenburg, Germany. The inset shows sensor and box location within one of the patches.**

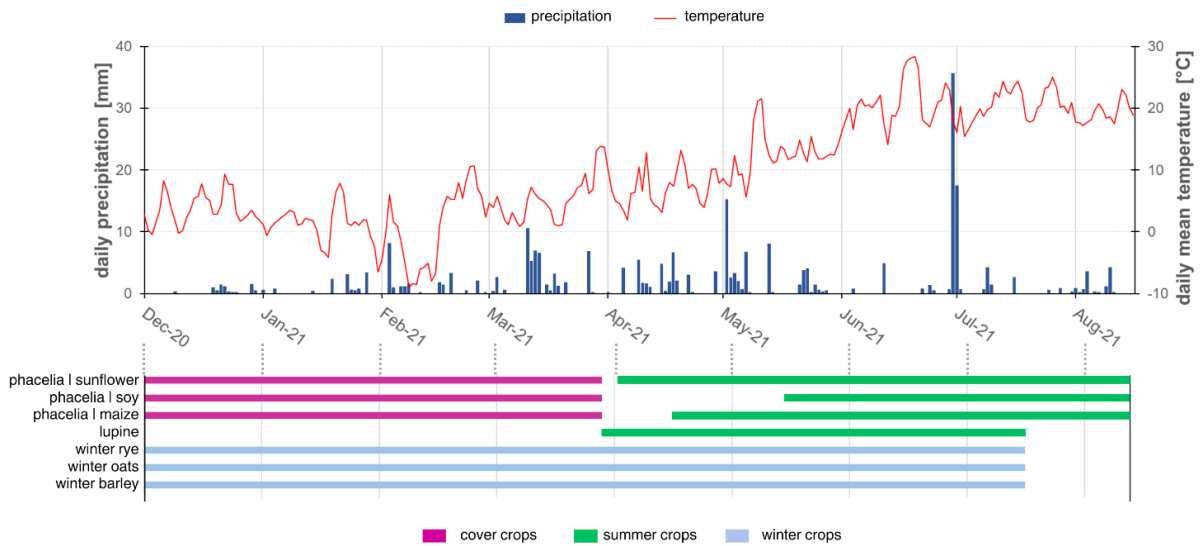
658



659

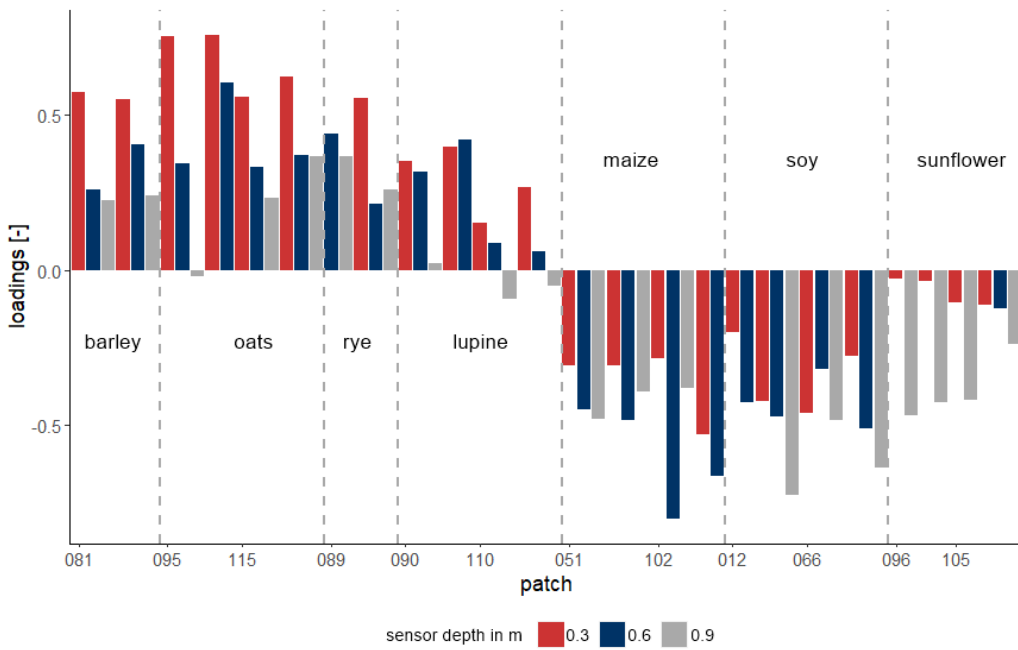
660  
661

**Figure 2: Input soil moisture time series per depth, differentiated between crop groups, and average soil moisture of all time series per depth from 2020-12-01 until 2021-08-15 at the patchCROP landscape laboratory, Tempelberg, Brandenburg, Germany.**



662

663 **Figure 3: Measured daily precipitation, mean temperature and cultivated crops - differentiated between winter crops (light blue**  
 664 **bars), summer crops (green bars) and cover crops (pink bars) - from 2020-12-01 until 2021-08-15 at the patchCROP landscape**  
 665 **laboratory, Tempelberg, Brandenburg, Germany. Specific crops for the studied timeframe stated at the left side of the horizontal**  
 666 **bars.**

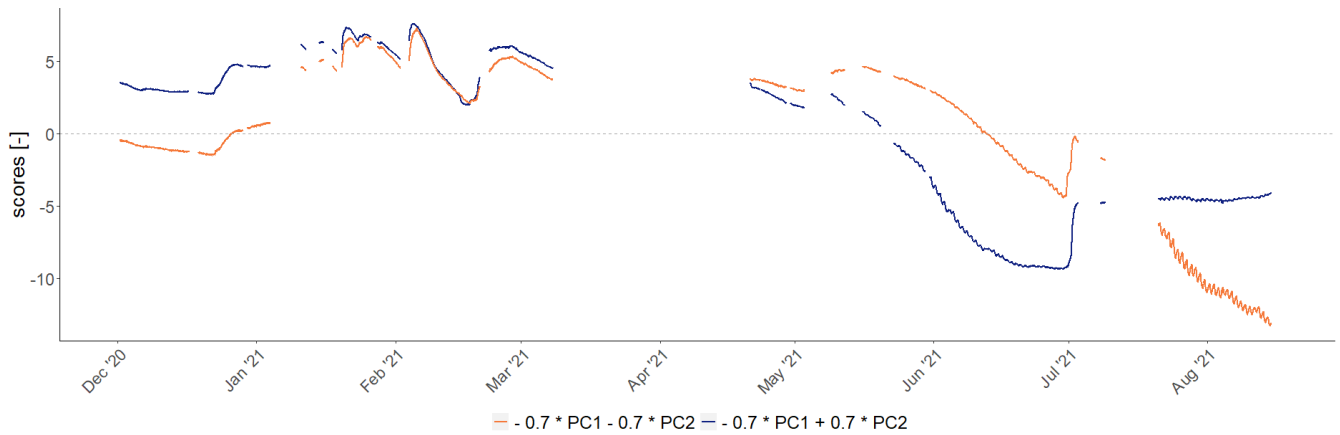


667

668

669 **Figure 4: Time series Loadingsloadings of time series on the second principal component at the patchCROP landscape laboratory,**  
 670 **Tempelberg, Brandenburg, Germany, showing a crop group related pattern.** Bars represent individual time series grouped by  
 671 **patch ID and sorted by crop.**

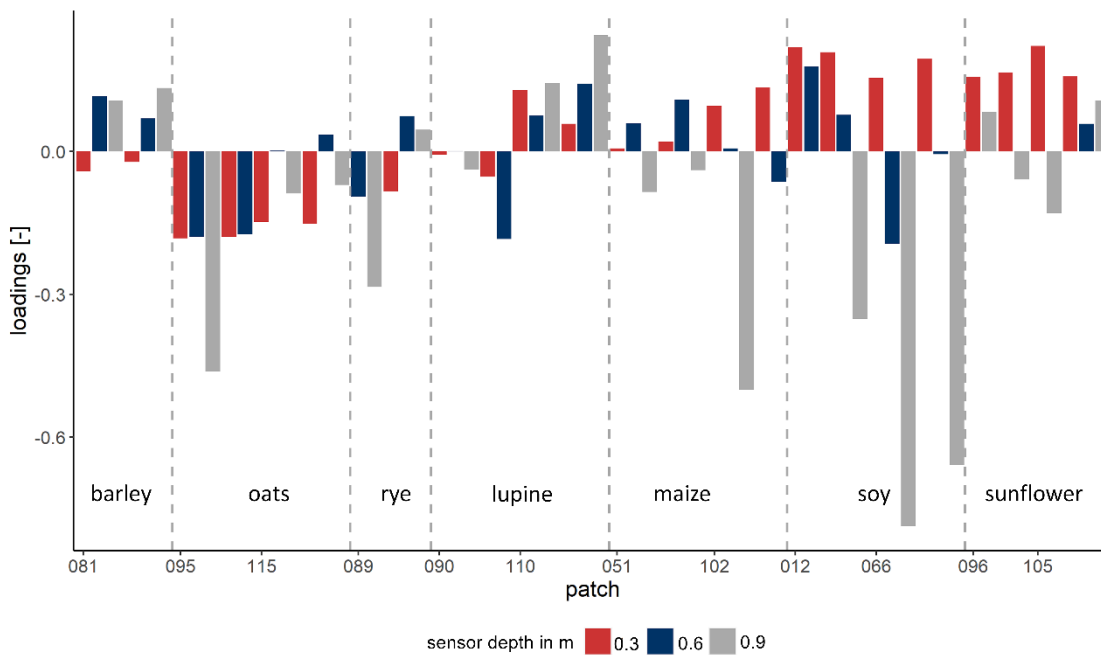
672



673

674 **Figure 5: Effect of the second principal component on modification of the general mean behaviour presented by the first principal**  
 675 **component at the patchCROP landscape laboratory, Tempelberg. The blue line represents deviations from mean soil moisture for**  
 676 **time series with positive loadings on PC2 (winter crops) while the orange line represents deviations from mean soil moisture for time**  
 677 **series with negative loadings on PC2 (summer crops).**

678

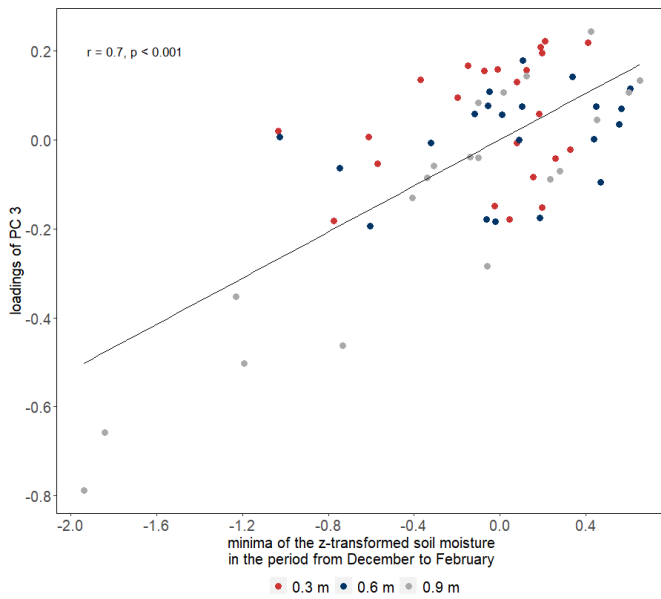


679

680

681 **Figure 6: Loadings of time series on the third principal component at the patchCROP landscape laboratory, Tempelberg,**  
 682 **Brandenburg, Germany with some of the sensors in deeper layers showing noticeably negative loadings.** Bars represent individual  
 683 **time series grouped by patch ID and sorted by crop.**

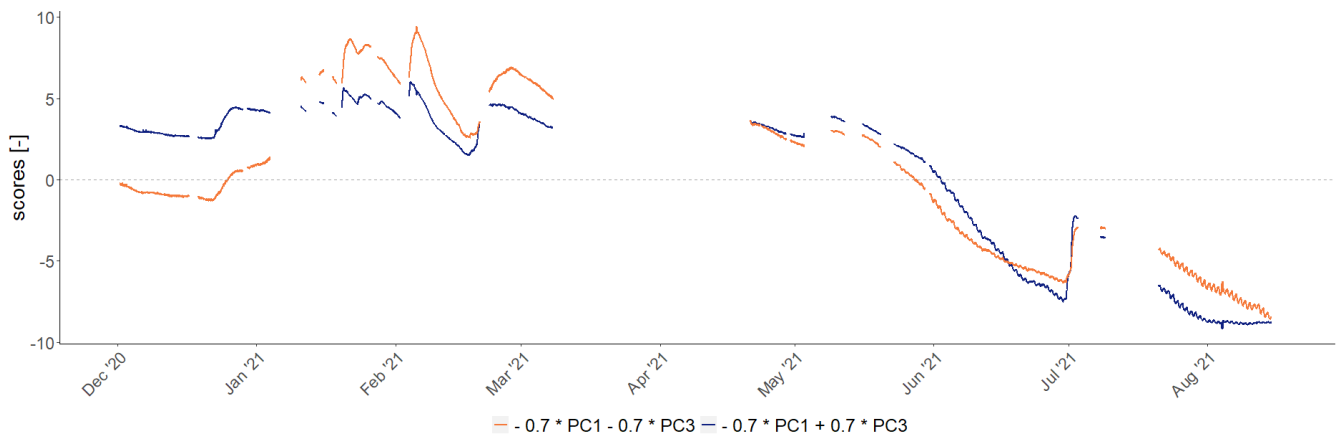




684

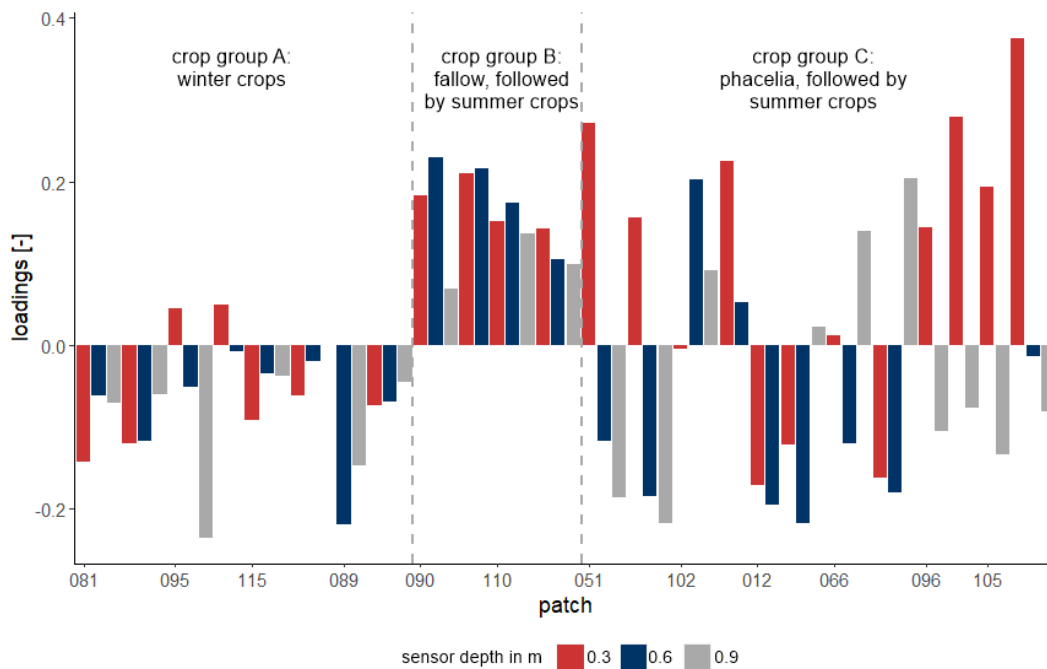
685 **Figure 7: Relation between minima of the z-transformed soil moisture in the first months of the study period with loadings of third**  
 686 **principal component showing that sensors with noticeably negative loadings showed distinctly negative z-transformed minima.**

687



688

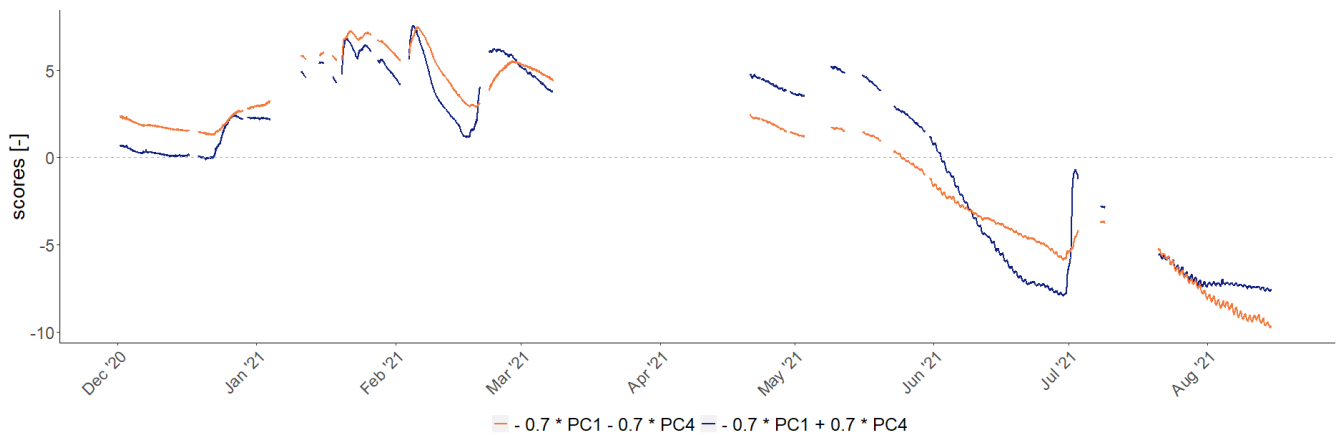
689 **Figure 8: Effect of the third principal component on modification of the general mean behaviour presented by the first principal**  
 690 **component at the patchCROP landscape laboratory, Tempelberg. The blue line represents deviations from mean soil moisture for**  
 691 **time series with positive loadings on PC3 (majority of the time series) while the orange line represents deviations from mean soil**  
 692 **moisture for time series with negative loadings on PC3 (part of the sensors in 0.9 m depth).**



694

695 **Figure 9: Loadings of time series on the fourth principal component at the patchCROP landscape laboratory, Tempelberg,**  
 696 **Brandenburg, Germany showing mainly negative loadings for crop group A, positive loadings for crop group B and loadings with**  
 697 **no clear pattern for crop group C. Bars represent individual time series grouped by patch ID, sorted by treatment group.**

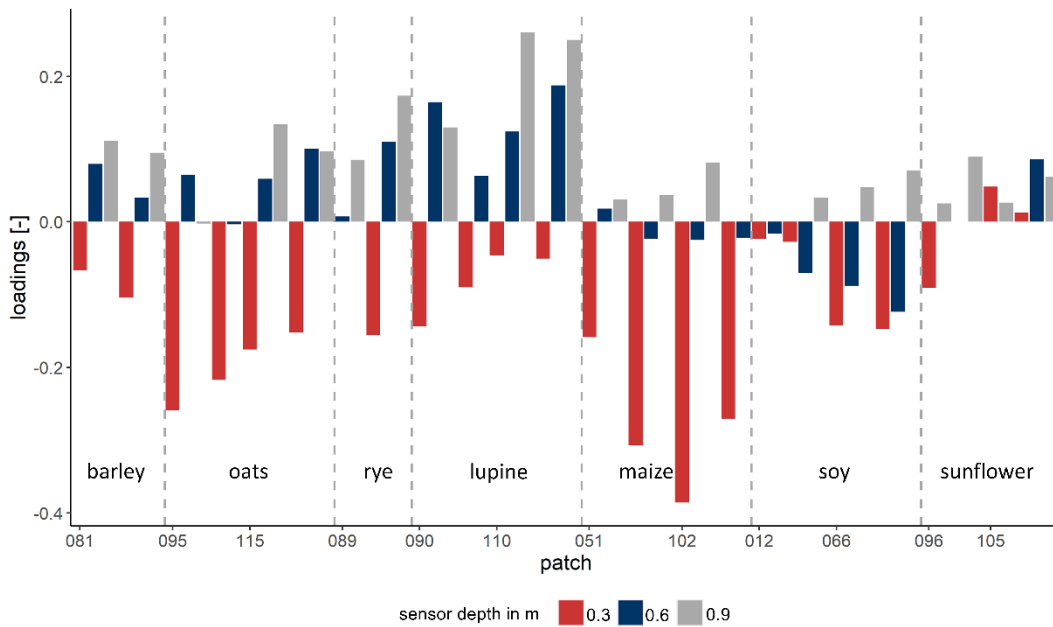
698



699

700 **Figure 10: Effect of the fourth principal component on modification of the general mean behaviour presented by the first principal**  
 701 **component at the patchCROP landscape laboratory, Tempelberg. The blue line represents deviations from mean soil moisture for**  
 702 **time series with positive loadings on PC4 (single sensors of crop group A, all sensors of crop group B, and part of crop group C)**  
 703 **while the orange line represents deviations from mean soil moisture for time series with negative loadings on PC4 (most sensors of**  
 704 **crop group A and part of the sensors of crop group C).**

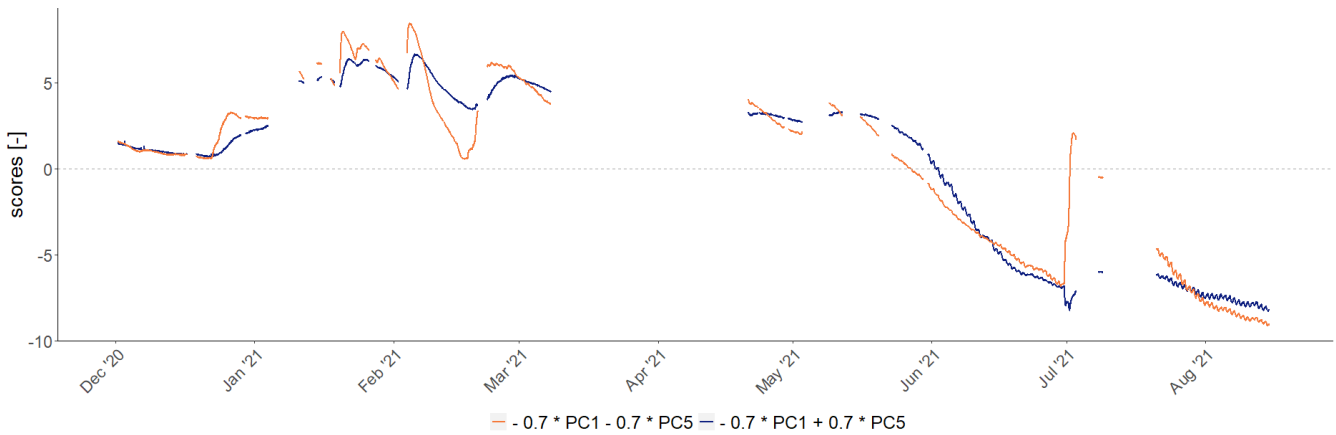
705



706

707 **Figure 11: Loadings of time series on the fifth principal component at the patchCROP landscape laboratory showing a depth**  
 708 **related pattern.** Bars represent individual time series grouped by patch ID, sorted by crop.

709



710

711 **Figure 12: Effect of the fifth principal component on modification of the general mean behaviour presented by the first principal**  
 712 **component at the patchCROP landscape laboratory, Tempelberg.** **The blue line represents deviations from mean soil moisture for**  
 713 **time series with positive loadings on PC5 (sensors in greater depth) while the orange line represents deviations from mean soil**  
 714 **moisture for time series with negative loadings on PC5 (sensors in shallow depth).**

715

716

717 Table 1: Overview of crop rotation, sand content in the top 0.25 m soil depth and weed control for selected of analysed patches at  
 718 the patchCROP landscape laboratory, Tempelberg, Brandenburg, Germany.

Crop in winter season	Crop in summer season	Crop group	Sand content (in 1 m buffer zone around sensors) in [%]	Weed control	Patch ID
<u>Winter barley</u>		<u>A</u>	<u>78.3</u>	<u>conventional</u>	81
Winter oats		A	80.7	conventional	95
Winter oats		A	80.6	reduced	115
Winter rye		A	80.5	conventional	89
Fallow	Lupine	B	80.6	conventional	90
Fallow	Lupine	B	80.3	reduced	110
Phacelia	Maize	C	80.8	reduced	51
Phacelia	Maize	C	80.6	conventional	102
Phacelia	Soy	C	78.5	reduced	12
Phacelia	Soy	C	77.9	conventional	66
Phacelia	Sunflower	C	80.6	conventional	96
Phacelia	Sunflower	C	80.5	reduced	105

719

720 Table 2: Overview of normalized difference vegetation index (NDVI), surface temperature, and slope at the locations of analysed  
 721 sensors at the patchCROP experiment in Tempelberg, Brandenburg, Germany.

Crop	Patch ID	Sensor Position	NDVI 2021-05-20 [-]	NDVI 2021-05-31 [-]	NDVI 2021-07-06 [-]	Surface Temperature <u>2021-05-31</u> in [°C]	Slope in [°]
<u>Winter B</u> barley	81	West	0.874	0.182	0.926	20.57	2.01
<u>Winter b</u> Barley	81	East	0.875	0.180	0.927	20.43	1.94
<u>Winter o</u> Oats	95	East	0.838	0.208	0.834	27.25	1.36
<u>Winter O</u> oats	95	West	0.838	0.213	0.840	27.85	1.15
<u>Winter o</u> Oats	115	West	0.756	0.278	0.845	23.70	1.28
<u>Winter O</u> oats	115	East	0.783	0.281	0.863	25.12	0.43
<u>Winter R</u> rye	89	West	0.796	0.263	0.856	22.39	1.74
<u>Winter r</u> Rye	89	East	0.787	0.206	0.822	24.95	1.67
Lupine	90	West	0.185	0.395	0.710	26.31	1.40
Lupine	90	East	0.203	0.391	0.733	24.96	1.27
Lupine	110	West	0.090	0.563	0.635	26.98	1.88
Lupine	110	East	0.090	0.567	0.639	26.76	2.50

Maize	51	West	-0.099	0.654	0.181	35.44	0.82
Maize	51	East	-0.096	0.638	0.217	35.29	0.93
Maize	102	West	-0.077	0.714	0.175	37.88	0.88
Maize	102	East	-0.058	0.728	0.178	38.03	0.90
Soy	12	West	-0.107	0.748	0.166	34.87	1.71
Soy	12	East	-0.108	0.723	0.162	34.44	1.11
Soy	66	West	-0.115	0.730	0.144	35.09	2.40
Soy	66	East	-0.114	0.661	0.147	34.39	2.13
Sunflower	96	West	-0.109	0.816	0.211	33.76	0.59
Sunflower	96	East	-0.101	0.827	0.229	34.70	0.69
Sunflower	105	West	0.178	0.610	0.564	29.79	1.04
Sunflower	105	East	0.030	0.696	0.399	34.53	1.00

722

723

724

**Table 3: Statistical characteristics and interpretations of principal components 1 to 5 for soil moisture dynamics of selected patches at the patchCROP landscape laboratory, Tempelberg, Brandenburg, Germany.**

	<b>PC1</b>	<b>PC2</b>	<b>PC3</b>	<b>PC4</b>	<b>PC5</b>
<b>Eigenvalue</b>	46.25	10.89	2.60	1.43	1.06
<b>Proportion of variance in %</b>	72.27	17.01	4.06	2.23	1.65
<b>Proportion of variance (cumulative) in %</b>	72.27	89.28	93.34	95.57	97.22
<b>Interpretation</b>	Mean behaviour	Winter vs. summer crops	Subsoil texture	<del>Soil organic carbon</del> <u>winter vegetation cover and influence of cover crops on soil</u>	Damping of the input signal
<b>Prevailing driver</b>	weather	crop	soil	crop and soil	soil

725

726

727

728

729

**Table 4: Pearson correlation coefficients between ~~drone imagery products~~surface temperature and normalized difference vegetation index (NDVI)-at the patchCROP landscape laboratory, Tempelberg, Brandenburg, Germany taken on May 31<sup>st</sup>, 2021, and loadings of sensors in all depths or at single depths, respectively, on the second principal component. All correlations -are were highly significant ( $p < 0.01$ ).**

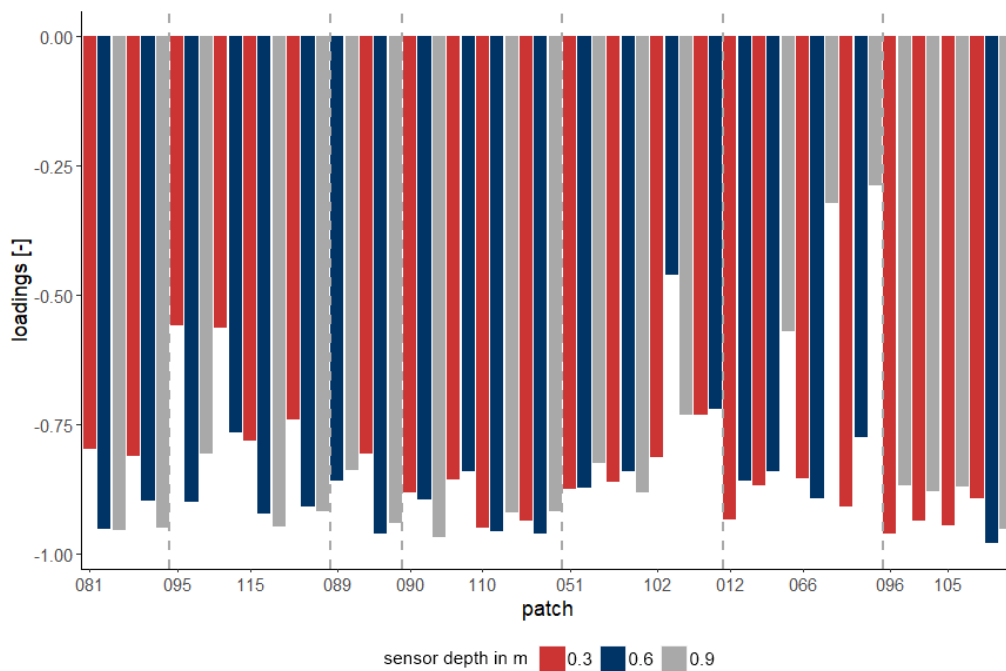
<u>Variable</u>	<b>Sensors in all depths</b>	<b>0.3 m</b>	<b>0.6 m</b>	<b>0.9 m</b>
<b>Surface temperature</b>	-0.853	-0.881	-0.909	-0.916

NDVI 2021-05-20	0.836	0.904	0.837	0.907
NDVI 2021-05-31	0.899	0.945	0.944	0.946
NDVI 2021-07-06	-0.860	-0.898	-0.917	-0.913

730

731

732 APPENDIX A



733

734 **Figure 13: Loadings of time series on the first principal component at the patchCROP landscape laboratory, Tempelberg,**  
735 **Brandenburg, Germany.** Bars represent individual time series grouped by patch ID and sorted by crop.

736